UNIVERSIDADE DE SÃO PAULO

INSTITUTO DE FÍSICA
CAIXA POSTAL 20516
01498 - SÃO PAULO - SP
BRASIL

PUBLICAÇÕES

IFUSP/P-583

MICROSCOPIC MULTIPLE SCATTERING THEORY OF THE HEAVY ION TOTAL REACTION CROSS SECTION

by

M.S. Hussein
Instituto de Física, Universidade de São Paulo

and

R.A. Rego
Divisão de Física Teórica, Instituto de Estudos Avançados, Centro Técnico Aeroespacial, 12200 São José dos Campos, SP, Brasil

Maio/1986

MICROSCOPIC MULTIPLE SCATTERING THEORY OF THE HEAVY ION TOTAL REACTION CROSS SECTION

M.S. Hussein*

Instituto de Física, Universidade de São Paulo,
C.P. 20516, 01498 São Paulo, S.P., Brasil

and

R.A. Rego

Divisão de Física Teórica, Instituto de Estudos Avançados, Centro Técnico Aeroespacial,
12200 São José dos Campos, S.P., Brasil

*Supported in part by the CNPq.

May/1986

CONTENTS

ABSTRACT

The multiple scattering theory is used to develop a theoretical framework for the calculation of the heavy-ion total reaction cross section. Several important medium effects such as Pauli blocking, are included. The second order double scattering contribution to the ion-ion "$t\rho_1\rho_2$" interaction is calculated and found to contribute at most 10% effect on σ_R. It is found that whereas at intermediate energies the "$t\rho_1\rho_2$" accounts reasonably well for the total reaction cross section, indicating the predominance, at these energies, of single nucleon knockout, it understimate σ_R at lower energies by a large amount. This is mainly due to the absence in "$t\rho_1\rho_2$" of fusion and inelastic surface excitation.

I. INTRODUCTION

In recent years the total reaction cross section of heavy ions has become the focus of extensive theoretical[1-6] and experimental[7-10] attention. On the theoretical side, microscopic calculations have been performed within both the $(t\rho_1\rho_2)$[2] Lax approximation and the more exact G-matrix formulation[4] A major emphasis has been allocated to the discussion of the degree of transparancy in the heavy ion system, and how this is traced to the nucleon-nucleus scattering. A basic input in these calculation is the nucleon-nucleon elastic t-matrix appropriately modified to take into account nuclear medium effects in both projectile and target.

Since at intermediate energies these medium effects can be taken into account as corrections added a posteriori to the free nucleon-nucleon t-matrix, one may use this exhaustively studied object in the calculation of σ_R. Owing to the linear relation involving the total nucleon-nucleon cross section and the Im t, through the optical theorem, the energy variation of σ_T^{NN} is accordingly quite relevant for the purpose. In particular the discussion of the reactive content of σ_R whether for nucleon--nucleus or nucleus-nucleus systems becomes intimately related to that of σ_T^{NN}.

To set the stage for action we show in Fig. (1) the already extensively exhibited σ_T^{NN} vs center of mass energy,

for the pp and pn systems[11]. We note that σ_T^{pn} about twice as large as σ_T^{pp} or σ_T^{pn} at small energies. At intermediate energies they become comparable. Ignoring the very small bremsstrahlung emission, the cross section σ_T^{pn} at E_L<280 MeV is practically 100% elastic scattering. The first reaction channel, namely one pion production, opens at $E_{Lab} \sim 280$ MeV, followed at $E_{Lab} = 530$ MeV by the two-pion production cross section, etc.. Thus in the energy range $0 < E < 280$ MeV the nucleon nucleon total reaction cross section is just the one-pion production cross section integrated over angle. This is shown in Figure (2).

In fact, what is plotted are the production cross sections for the isospin T=1 and T=0 states. The identifications $\sigma_R(T=1) = \sigma_R^{pp}$ and $\sigma_R(T=0) = 2\sigma_R^{np} - \sigma_R^{pp}$ then give the relevant nucleon-nucleon cross section. As a result, one finds, at least in the energy regime $E_n < 580$ MeV (i.e. before reaching the two pion production threshold), that σ^{np} is about 0.62% of σ_R^{pp}. For the purpose of completeness, we also show, in Fig.(3), the two pion production cross-sections $\sigma(np \to np\pi^+\pi^-)$ and $\sigma(pp \to pp\pi^+\pi^-)$. These cross sections are orders of magnitude smaller than the one-pion production cross-section.

Clearly, the threshold energies for one-, and two-pion production processes in the free nucleon-nucleon system are significantly reduced in magnitude in the nucleon-nucleus and more so in the nucleus-nucleus systems, owing to nuclear

medium effects as recent experimental findings have shown[12]. This fact, however does not necessarily indicate that qualitative considerations concerning the reactive context of nucleon-nucleus ($t\rho$), and nucleus-nucleus ($t\rho_1\rho_2$) interactions, respectively, cannot be made using as a guideline the nucleon-nucleon reaction cross sections discussed so far.

Accordingly we can afirm that the reactive content of the $t\rho$ and $t\rho_1\rho_2$ interactions is predominantly single nucleon knockout[13] at low energies, and/or one- or two-pion production at intermediate energies. Clearly the excitation of collective degrees of freedom are not accounted for in either of the interactions mentioned above. Thus it becomes quite important to investigate the energy range in which the "$t\rho_1\rho_2$" interaction is the dominant component of the ion-ion potential.

The vehicle through which the above can be accomplished is the multiple scattering description. This theory, not only supplies a convenient framework through which the simple Lax potential can be derived and discussed, but it also makes possible the construction of higher order corrections which may contribute significantly to σ_R at lower energies.

It is the purpose of this Report to investigate the significance of the "$t\rho_1\rho_2$" interaction for the total reaction cross section of heavy ions. Both nuclear medium effects and higher-order, multiple scattering contributions, are discussed. The principal aim is to discover the energy range in which this

interaction (at least its reactive content), approximates well, the interaction between two nuclei. Recent studies[2], have suggested that even at low energies ($E < 15 \frac{MeV}{N}$) the "$t\rho_1\rho_2$" interaction reproduces well the total reaction cross section. As we shall see later in this Report this is not so on account of the fact that several important reaction channels, not accounted for by the "$t\rho_1\rho_2$" potential, whose major reactive channel is single-nucleon knockout in both projectile and target nuclei, become increasingly important as the energy is lowered.

The organization of this Report is as follows: In Chapter II we present a detailed account of the theory of σ_R. In particular we discuss several approximations used for its evaluation. We also generalize the one-channel theory of σ_R to multichannels. Further, we assess the importance of using a relativistic Dirac description of the ion-ion elastic scattering through which σ_R can be calculated. The details of this latter generalization is collected in an appendix. In Chapter III we present a summary of the multiple scattering theory appropriate to heavy ion collisions.

The first-order "$t\rho_1\rho_2$" interaction as well as the second order double scattering contributions are then derived and analyzed. The imaginary part of the "$t\rho_1\rho_2$" interaction is then fully discussed in Chapter IV. A very careful analysis of the Pauli blocking in the context of heavy ions is also presented in this Chapter. Calculation of σ_R for several HI systems

is then presented in Chapter V, with a comparison with the data made for $^{12}C+^{12}C$. The effect of the identity of the particles on σ_R is also discussed. Finally, in Chapter VI, several concluding remarks are presented.

A number of appendices relevant for the discussion presented in the different Chapters of the Report are collected at the end.

II. THEORY OF THE TOTAL REACTION CROSS-SECTION

In this Section we present the full details of the theoretical structure of the total reaction cross section. The relation between σ_R and the underlying imaginary part of the optical potential is most generally and easily obtained using the generalized optical theorem. This we do first. We then turn to the discussion of σ_R within several limiting cases and approximations, in particular the eikonal expression for σ_R is fully investigated.

Let us first consider the Lippmann-Schwinger Equation for the optical T-matrix which describes elastic scattering

$$T = V + V G_0^{(+)}(E)\, T \qquad \text{(II.1)}$$

where $G_0^{(+)}$ is the free propagator or Green function $= (E - H_0 + i\varepsilon)^{-1}$ with H_0 being the free Hamiltonian. In Eq. (II.1), V denotes the complex optical potential.

We multiply Eq. (II.1) from the right by T^{-1} and from left by V^{-1} to obtain

$$V^{-1} = T^{-1} + G_0^{(+)}(E) \qquad \text{(II.2)}$$

Applying the same procedure for the complex conjugate version of (II.1) gives

$$V^{\dagger} = T^{\dagger\,-1} + G_0^{(-)}(E) \qquad \text{(II.3)}$$

Subtracting (II.3) from (II.2) results in the following

$$T^{-1} - T^{\dagger\,-1} = V^{-1} - V^{\dagger\,-1} + 2\pi i\, \delta(E - H_0) \qquad \text{(II.4)}$$

the last term in Eq. (II.4) is just the difference $G_0^{(+)}(E) - G_0^{(-)}(E)$. We now multiply Eq. (II.4) from the left by $T^{\dagger}$ and from the right by T to get, after using the relations $T = V\Omega^{(+)}$ and $T^{\dagger} = \Omega^{(+)\dagger} V^{\dagger}$ when $\Omega^{(+)}$ is the Möller wave operator,

$$T - T^{\dagger} = \Omega^{(+)\dagger}(V - V^{\dagger})\,\Omega^{(+)} - 2\pi i\, T^{\dagger}\delta(E - H_0)\, T \qquad \text{(II.5)}$$

We are now in a position to derive the optical theorem which relates the imaginary part of the forward scattering amplitude to the total cross section. Indeed, taking the on-shell matrix element (in plane waves) of (II.5) leads, immediately to (k'=k)

$$\mathrm{Im}\; T^{\text{on-shell}}(k, o^{\circ}) = \frac{1}{2i}\langle \vec{k}|\Omega^{(+)\dagger}(V - V^{\dagger})\,\Omega^{(+)}|\vec{k}\rangle$$

$$= \frac{1}{2i}\,\frac{2\pi i\,\mu k}{(2\pi)^3\hbar^2}\int d\Omega_{\hat{k}'}\left| T^{\text{on-shell}}\left(\vec{k}', \vec{k}, \frac{\hbar^2 k^2}{2\mu}\right)\right|^2 \qquad \text{(II.6)}$$

Using now the relation between $T^{\text{on-shell}}$ and the elastic

scattering amplitude f ,

$$f(k,\theta) = -\frac{\mu}{2\pi\hbar^2} T^{\text{on-shell}}(k,\theta) \qquad \text{(II.7)}$$

we obtain

$$\frac{4\pi}{k} \mathrm{Im}\, f(k,0) = \frac{k}{E_k} \langle \Psi^{(+)}_{\vec{k}} | \mathrm{Im} V | \Psi^{(+)}_{\vec{k}} \rangle + \int d\Omega \left| f(k,\theta) \right|^2 \qquad \text{(II.8)}$$

which is the generalized optical theorem we are seeking. Since on the righ-hand side, we have the total cross-section, and $\int d\Omega \frac{d\sigma_{e\ell}}{d\Omega}$ is the angle integrated elastic cross section, we can immediately identify the first term on the right-hand-side to be just the total reaction cross section

$$\sigma_R = \frac{k}{E_k} \langle \Psi^{(+)}_{\vec{k}} | \mathrm{Im} V | \Psi^{(+)}_{\vec{k}} \rangle \qquad \text{(II.9)}$$

In the above derivation of σ_R through the use of the optical theorem, we did not pay attention to the long range Coulomb interaction. This, however, poses no fundamental problem as one can generalize the optical theorem, in such a way as to have $\mathrm{Im}[f(0) - f_{\text{Ruth}}(0)]$ on the left-hand side of Equation (II.8) and $\int d\Omega \left[|f(k,\theta)|^2 - |f_{\text{Ruth}}(k,\theta)|^2 \right]$ as the second term on the right hand side of the same equation. In the above expressions, $f_{\text{Ruth}}(0)$ is the Rutherford scattering amplitude. The first

term, namely σ_R (see Equation (II.9)), is unchanged. For full details of the above generalization we refer the reader to Haldeman and Thaler[11] and Hussein et. al.[12]. For completeness, an alternative, more direct, derivation of σ_R using the usual Wronskian argument is presented in Appendix I.

Equation (II.9) can be straightforwardly partial-wave expanded yielding

$$\sigma_R = \frac{\pi}{k^2} \sum_{\ell=0}^{\infty} (2\ell+1) T_\ell \qquad \text{(II.10)}$$

with the elastic channel transmission coefficients T_ℓ, given by

$$T_\ell = \frac{8\mu k}{\hbar^2} \int_0^\infty dr \left| \psi_\ell(k,r) \right|^2 \left| \mathrm{Im} V(r) \right| \qquad \text{(II.11)}$$

where $\psi_\ell(k,r)$ is the exact partial wave, radial, wave function, which is a solution of the radial optical Schrödinger equation (with the full V). Of course the following relation holds between T_ℓ and the elastic S-matrix

$$T_\ell = 1 - |S_\ell|^2 \qquad \text{(II.12)}$$

In the large-number-of-partial-waves limit, and under semiclassical conditions, one may replace the partial wave sum by an integral and ℓ by $kb - \frac{1}{2}$, with b being

the impact parameter. Thus Eq. (II.10) becomes

$$\sigma_R = 2\pi \int_0^\infty b\, db\, T(b) \tag{II.13}$$

In the application to heavy ion reactions, it has been customarily to introduce a strong absorption radius $R_{s.a.}$ which would limit the b-integral above in the sense that $T(b)$ is represented as

$$T(b) = \Theta(R_{s.a.} - b) \tag{II.14}$$

Eq. (II.14) implies the limit of infinite absorption (large ImV) for $b < R_{s.a.}$ and zero absorption for $b > R_{s.a.}$, a case hardly exactly met in physical systems. It does, however, constitutes a reasonable first approximation for $T(b)$. It is important here to remind the reader that $R_{s.a.}$ is energy dependent to account for the Coulomb barrier restriction. Usually $R_{s.a.}$ is taken to be

$$R_{s.a.} = R_B\left(1 - \frac{V_B}{E}\right)^{1/2} \tag{II.15}$$

where R_B and V_B are the position and height of the Coulomb barrier, and E is the center of mass energy. With (II.15), σ_R becomes

$$\sigma_R = \pi R_B^2\left(1 - \frac{V_B}{E}\right) \tag{II.16}$$

The above expression for σ_R, does account well for heavy ion total reaction cross section data up to center of mass energy per nucleon about one fourth the Fermi energy (ε_F = 37 MeV). At higher energies, the data start dropping off until an $\frac{\text{energy}}{N}$ of about 140 MeV (roughly equal to the pion rest mass) is reached after which σ_R rises again. This fact clearly shows that a great amount of transparancy is attained at intermediate energies, and the question arises as how to relate the transparancy to more fundamental physical quantities, such as the nucleon-nucleon total cross section. The vehicle through which this is accomplished is the explicit connection between $T(b)$ of Eq. (II.13) and the elastic channel optical potential, as Eq. (II.11) implicitly dictates. The optical potential itself is constructed from multiple scattering theory as will be discussed in Section III.

In terms of the complex phase shift which specifies, S, namely $S = \exp(2i\delta)$, we may write

$$T(b) = 1 - \exp\left(-4\,\delta_I(b)\right) \tag{II.17}$$

where $\delta_I(b) = \mathrm{Im}\,\delta(b)$. Within the J.W.K.B. approximation, we have for the phase shift

$$\delta_\ell = \lim_{r\to\infty}\left[\int_{r_1}^{r} dr' \sqrt{\left(k^2 - \frac{\ell(\ell+1)}{r'^2} - \frac{2\mu}{\hbar^2}V(r)\right)} - \int_{r_0}^{r} dr' \sqrt{k^2 - \frac{\ell(\ell+1)}{r'^2}}\right] \qquad \text{(II.18)}$$

where r_1 is the turning point, and $r_0 \equiv \frac{\ell+\frac{1}{2}}{k} = b$. The imaginary part of δ_ℓ is obtained immediately

$$\delta_I(\ell) = \int_{r_1}^{\infty} dr' \sqrt{\left[k^2 - \frac{\ell(\ell+1)}{r'^2} - \frac{2\mu}{\hbar^2}\,Re\,V(r')\right]^2 + \left(\frac{2\mu}{\hbar^2}\,Im\,V(r')\right)^2} \cdot \sin\left(\frac{\theta(r')}{2}\right) \qquad \text{(II.19)}$$

where

$$\tan\theta(r') = \frac{-\frac{2\mu}{\hbar^2}\,Im\,V(r')}{\left[k^2 - \frac{\ell(\ell+1)}{r'^2} - \frac{2\mu}{\hbar^2}\,Re\,V(r')\right]} \qquad \text{(II.20)}$$

At sufficiently high energies, in the sense of $V/E < 1$, one may expand (II.19) to first order in $Im\,V$, to obtain

$$\delta_I = -\frac{1}{2}\,\frac{2\mu}{\hbar^2}\int_{r_1}^{\infty} dr' \frac{Im\,V(r')}{\left[k^2 - \frac{\ell(\ell+1)}{r'^2} - \frac{2\mu}{\hbar^2}\,Re\,V(r')\right]^{1/2}} \qquad \text{(II.21)}$$

which may be considered as a precursor of Glauber (or the Eikonal) formula, since with the use of cylindrical coordinates $r' = (z,b)$ and ignoring $Re\,V(r')$ in the square root, one may write

$$\delta_I(b) = -\frac{1}{4}\,\frac{2\mu}{\hbar^2 k}\int_{-\infty}^{\infty} dz'\; Im\,V\left(\sqrt{b^2+z'^2}\right) \qquad \text{(II.22)}$$

The above expression is to be contrasted with that given in Eq. (II.21), in that the former involves a free trajectory for the incident particle (using classical language) whereas the latter moves on a trajectory determined by the combined Coulomb plus $Re\,V(r)$ potentials.

We note that $\delta_I(b)$ should behave as a function of impact parameter, similarly to that of $Im\,V(b)$. In fact, if we make the approximation $Im\,V = -W_0\,\theta(R-r')$, we obtain

$$\delta_I(b) = \frac{k}{2E}\,W_0\sqrt{R^2-b^2}\;\theta(R-b) \qquad \text{(II.23)}$$

The difference between (II.23) and that obtained with a Wood-Saxon form for $Im\,V$ is concentrated at the surface region,

The transmission coefficient $T(b)$, Eq. (II.17) is then given by

$$T(b) = 1 - exp\left[-\frac{2kW_0}{E}\sqrt{R^2-b^2}\;\right] \qquad \text{(II.24)}$$

It is clear from the above formula that the dependence of $T(b)$ on E and consequently that of σ_R is determined from the dependence of W_0 on E. If $W_0 \propto E^{\frac{1}{2}}$, the energy dependence of $T(b)$ is washed out. On the other hand if $W_0 \propto E^{\frac{1}{2}} \sigma_{NN}(E)$, then the energy-dependence of $T(b)$ is exclusively determined by the energy dependence of $\sigma_{NN}(E)$, as will be fully discussed later. Obviously, the above simple rule, changes as the energy is lowered, since an extra energy-dependence will emerge from the factor $\left(k^2 - \frac{l(l+1)}{r^2} - \frac{2\mu}{\hbar^2} Re\, V(r)\right)^{-1/2}$ in Eq. (II.21). Further, nuclear medium effects, e.g. Pauli blocking, introduces further energy dependence. These questions will be fully addressed in the next section.

Though very schematic, the expression obtained for $T(b)$, Eq. (II.24) using the square well model for $Im\, V(r)$, still serves to exhibit several interesting features of σ_R. Using Eq. (II.24) in Eq. (II.13), we obtain for $\sigma_R(E)$

$$\sigma_R(E) = \pi R^2 \left[1 - 2\,\frac{1-(1+2R/\lambda)\,e^{-2R/\lambda}}{(2R/\lambda)^2}\right] \qquad \text{(II.25)}$$

where $\lambda = \frac{E}{kW_0}$ is the mean free path. This equation was first derived by Bethe[15]. To correct for the Coulomb barrier effect one merely replaces (II.25) by[16]

$$\sigma_R(E) = \pi R_E^2 \left[1 - 2\,\frac{1-(1+2R_E/\lambda)\,e^{-2R_E/\lambda}}{(2R_E/\lambda)^2}\right] \cdot \left(1 - \frac{V_B}{E}\right) \qquad \text{(II.26)}$$

where $R_E = R + \frac{1}{k}$.

Equation (II.26) may be compared with the purely geometrical formula (II.16) and thus the transparancy factor, T, defined by

$$\sigma_R = \pi R_E^2 \left(1 - T\right)\left(1 - \frac{V_B}{E}\right) \qquad \text{(II.27)}$$

can be immediately extracted

$$T = 2\,\frac{1-(1+2R_E/\lambda)\,e^{-2R_E/\lambda}}{(2R_E/\lambda)^2} \qquad \text{(II.28)}$$

Figure (4) exhibits the behaviour of T vs $\frac{2R_E}{\lambda}$

Eq. (II.28) identifies the physical parameter that determines the value of T, namely $\left(\frac{2R_E}{\lambda}\right)$. For large $\frac{2R_E}{\lambda}$, namely $\lambda \ll 2R_E$, we obtain for T,

$$T \approx \lambda^2 / 2R_E^2 \qquad \text{(II.29)}$$

and accordingly, the total reaction cross-section becomes proportional to the surface

$$\sigma_R \sim \pi R_E^2 \left(1 - \frac{\lambda^2}{2R_E^2}\right)\left(1 - \frac{V_B}{E}\right)$$

$$\propto A^{2/3} \quad \text{for nucleon-induced reaction} \qquad \text{(II.30)}$$

$$\propto \left(A_1^{1/3} + A_2^{1/3}\right)^2 \quad \text{for ion-ion collisions}$$

The above result is characteristic of strongly interacting systems characterized by short λ such as hadron-nucleus. On the other hand in the other extreme, namely $\frac{2R_E}{\lambda} << 1$ (implying long mean free path λ compared to the effective diameter of the interacting system), we obtain

$$T \approx 1 - \frac{2}{3}\left(\frac{2R_E}{\lambda}\right), \qquad \text{(II.31)}$$

giving thus for the total reaction cross section the following from which is proportional to the effective volume of the system

$$\sigma_R \sim \left(\frac{4\pi}{3} R_E^3\right) / \lambda \quad \text{for a nucleon-induced reaction} \qquad \text{(II.32)}$$

$$\propto A \quad \text{for ion-ion collisions}$$

$$\propto \left(A_1^{1/3} + A_2^{1/3}\right)^3$$

The A-behaviour of σ_R in Eq. (II.32) is typical of weakly interacting probes with a nuclear target. Examples are electron- and photon-induced reactions. The mean free path in these cases is quite long owing to the weakness of the underlying electro-

magnetic interaction. Accordingly, the whole nucleus is "seen" in the process of the collision, in contrast to hadron-induced reactions, where only the surface nucleons participate in the collision process.

Clearly, the above picture depends on energy, in the sense that weakly interacting probes behave, at higher energies, like hadrons (in the photo-nuclear case this is commonly referred to as the vector-meson-dominance phenomenon [8]). It seems obvious now (Eq. (1)) that very hadron-like processes, such as the ion-ion collision discussed here, behave at intermediate energies, like weakly interacting systems owing to the diminishing value , at these energies, of the total nucleon-nucleon cross section, the basic microscopic quantity for these systems. In the next sections we investigate, within more realistic calculations, the behaviour of σ_R and T as a function of the combined radius of the heavy-ion system.

So far we have discussed the total reaction cross section within a one-channel (optical) description of the elastic scattering process. In many instances, a more general description of nuclear absorption, based on coupled channels theory, is called for. Thus, in the following we present such a description for the purpose of completeness and in order to develop a theoretical framework through which improvements upon the multiple scattering calculation, presented in the bulk of this paper, can be eventually made.

We introduce now the projection operators, P_0, P' and Q, which project out, respectively, the elastic channel, the directly coupled nonelastic channels and the closed channels (fusion). The elimination of the Q-subspace and the energy average performed subsequently, results in an effective P_0+P' coupled channels. The aim now is to evaluate the total reaction cross section in P_0.

The equation for the elastic element of the T-matrix becomes now instead of Eq. (II.1)

$$P_0 T_1 P_0 = P_0 V P_0 + P_0 V P' G_0^{(+)} P' T P_0 \qquad \text{(II.33)}$$

which may also be written in the following equivalent form

$$P_0 T P_0 = U_{opt.} + U_{opt.} P_0 G_0^{(+)} P_0 T P_0 \qquad \text{(II.34)}$$

$$U_{opt.} = P_0 V P_0 + P_0 V P' G^{(+)} P' V P_0 \qquad \text{(II.35)}$$

when $P'g^{(+)}P'$ is the effective, exact propagator in the P'-subspace.

Of course the discussion presented earlier following Eq. (II.1) can be immediately applied to Eq. (II.34), with the only difference that the structure of the effective optical potential operator U_{opt} is now fully exhibited in Eq. (II.35). Using Eq. (II.35) in (II.5), which we write now as

$$P_0 (T - T^\dagger) P_0 = P_0 \Omega^{(+)\dagger} P_0 (U_{opt.} - U_{opt}^\dagger) P_0 \Omega^{(+)} P_0 - 2\pi i P_0 T^\dagger P_0 \delta(E - H_0) P_0 T P_0 \qquad \text{(II.36)}$$

we have

$$P_0 (T - T^\dagger) P_0 = P_0 \Omega^{(+)\dagger} P_0 (U_{opt.} - U_{opt.}^\dagger) P_0 \Omega^{(+)} P_0 + P_0 \Omega^{(+)\dagger} P_0 (V P' g^{(+)} P' V P_0 - (P_0 V P' g^{(+)} P' V P_0)) \Omega^{(+)} P_0 - 2\pi i P_0 T^\dagger P_0 \delta(E - H_0) P_0 T P_0 \qquad \text{(II.37)}$$

Assuming now that the P_0P' coupling interaction is Hermitian $V_{P'P_0} = (V_{P'P_0})^\dagger$, which is a reasonable approximation if we consider that the effect of the averaged out Q-space results mostly in an imaginary contribution to the diagonal terms, $U_{P_0P_0}$ and $U_{P'P'}$ (which appears in II.34), have, for the second term on the RHS of Eq. (II.37), the following

$$P_0 \Omega^{(+)\dagger} P_0 V P (P g^{(+)} P - P g^{(+)\dagger} P) P V P_0 \Omega^{(+)} P_0 = P_0 \Omega^{(+)\dagger} P_0 V P \left[-2\pi i \sum_{P_\beta} |\psi_{P_\beta}^{(-)}\rangle\langle\psi_P^{(-)}| + P g^{(+)\dagger} P (U_{opt} - U_{opt}^\dagger) g^{(+)} P \right] V P_0 \Omega^{(+)} P_0 \qquad \text{(II.38)}$$

The above result is a consequence of an identity satisfied by the Green function $P g^{(+)} P$. Using the fact that the Möller

operator defining the channels p' is

$$p\,\Omega^{(+)}\,p \;=\; p\,\varphi^{(+)}\,p\;V\,P_o\,\Omega^{(+)}\,P_o \qquad \text{(II.39)}$$

we can now write for $T_{p_o} - T^{\dagger}_{p_o}$, Eq. (II.36), the following expression

$$\begin{aligned} T - T^{\dagger} \;=\; & P_o\,\Omega^{(+)\dagger}\,P_o\,(\,U_{opt} - U^{\dagger}_{opt})\,P_o\,\Omega^{(+)}\,P_o \\ & + P_p\,\Omega^{(+)\dagger}\,P\,(\,U_{opt} - U^{\dagger}_{opt})\,P\,\Omega^{(+)}\,P \\ & - 2\pi i \sum_{p} P_o\,\Omega^{(+)\dagger}\,P_o\,V\,P\,|\psi^{(-)}_{p}\rangle\,\delta(E - H_{p_o})\,\langle\psi^{(-)}_{p}|\,P\,V\,P_o\,\Omega^{(+)}\,P_o \\ & - 2\pi i\; P_o\,T^{\dagger}\,P_o\,\delta\,(E - H_Q)\,P_o\,T\,P_o \end{aligned} \qquad \text{(II.40)}$$

The derivation of the total reaction cross section can now be accomplished using exactly the same steps followed in deriving Eq. (II.9). Then

$$\sigma_R \;=\; \frac{k}{E_k}\left[\langle\psi^{(+)}_{P_o}\,|\,\mathrm{Im}\,U^{(P_o)}_{opt}\,|\,\psi^{(+)}_{P_o}\rangle + \sum_{p}\langle\psi^{(+)}_{p}\,|\,\mathrm{Im}\,U^{(p)}_{opt}\,|\,\psi^{(+)}_{p}\rangle\right] + \sigma_D \qquad \text{(II.41)}$$

where σ_D represents the direct reaction contribution to σ_R and corresponds to the third term on the RHS of Eq. (II.40). The first term in the above equation represents absorption in the p_o and p' channels owing to coupling to the closed

channel subspace and thus corresponds to fusion. The above general expression for the fusion cross section has recently been used in discussing heavy ion fusion at low energies where coupled channels effects seem to be important[19-21].

Clearly Eq. (II.41) is, in principle, equivalent to Eq. (II.9), as long as the optical potential used in the latter represents the exact interaction in the elastic channel. The decomposition of σ_R into two distinct terms, namely σ_F and σ_D is, however, quite useful in discussing the reactive content of microscopically derived optical potentials. The "$t\rho_1\rho_2$" interaction analysed fully in the following Chapters represents but one term in σ_D. This may well be the dominant term at intermediate and high energies. However, at lower energies, we expect that σ_F and the other terms in σ_D such as inelastic channels, to be by far the dominant terms in σ_R. The derivation of the above result using the Wronskian is presented in Appendix I.

To end this Chapter, we comment briefly on the possible need of using a relativistic description of heavy-ion elastic scattering especially at $E_{C.M.}/A > 200$ MeV, where recent research in proton-nucleus scattering seem to indicate the starting point in such a description in the optical Dirac equation with a combined scalar and time component vector potentials employed as an interaction[22].

Our aim here is to assess the importance of the

relativistic effects on σ_R. For the purpose we have evaluated σ_R for proton scattering on ^{40}Ca and ^{208}Pb[23]. The details of this calculation is presented fully in Appendix III. Our results indicate very little difference between the relativistic and non-relativistic σ_R,s. We therefore reach the conclusion that a non-relativistic calculation of σ_R for heavy ions at energies up to $E_{C.M.}/A$ = 800 MeV, should be quite adequate. In Section III we discuss in detail the non-relativistic "$t\rho_1\rho_2$" interaction.

III-1. THE PROTON-NUCLEUS "$t\rho$" INTERACTION

In this sub-section we discuss in great details the microscopic nucleon-nucleus optical potential. We do this for two reasons. The first is that this interaction has been the subject of intensive theoretical investigation for more than 25 years, which resulted in a quite satisfactory status, and the second being that, in principle, the nucleus-nucleus optical potential, can be defined in terms of the nucleon-nucleus interaction through a folding integral (single folding). Of particular interest is the discussion of the reactive content of the nucleus-nucleus interaction, given the structure of the underlying nucleon-nucleus optical potential. This is important for a better understanding of the nature of the total HI reaction cross section at intermediate energies, which has received great attention recently.

A simple,first trial, guess at the form of the nucleon-nucleus potential is the classical relation

$$U(\vec{r}) = \int d\vec{r}\,' \; \rho(\vec{r}\,') \; V(\vec{r},\vec{r}\,')$$

where $V(r',r)$ is a properly antisymmetrized projectile nucleon-target nucleon interaction and $\rho(r')$ is the single particle (classical) density of the target nucleus (obtained from e.g. Hartree-Fock calculation). Clearly the above expression is not entirely

correct since, firstly, U is real whereas the optical potential must be complex to account for the non-elastic processes, and secondly, V(r,r') cannot be used as it contains singular components (the "hard core") at $r < 0.4$ fm. What is used instead of V(r,r') is an appropriate effective potential, (or G-matrix) whose hard core is smoothed out, in favor of density dependence (absent in V(r,r')).

An apparently different method, usually applied at higher energies is to formulate the problem within a multiple scattering framework. Here one has as an input, the nucleon-nucleon t-matrix (generally off the energy shell). In this paper, we use this latter approach, both in nucleon- and nucleus-nucleus scattering. For the purpose of completeness, and the presentation of a general framework, where correction to first order approximation may be constructed and discussed, we present below the essential ingredients of this approach[24].

The Hamiltonian for the projectile nucleon-target nucleus system is written as,

$$H = -\frac{\hbar^2}{2m}\vec{\nabla}^2 + H_N + V \qquad \text{(III.1)}$$

where H_N is the target nucleus Hamiltonian and V is the interaction between the incident nucleon and the target nucleus, which can be written as a sum of individual nucleon-nucleus interactions

$$V = \sum_{i=1}^{A} V_{pi} \qquad \text{(III.2)}$$

The solution of the scattering problem is represented by the full nucleon-nucleus T-matrix

$$T = V + V\frac{}{E-(H-V)+i\varepsilon}T \qquad \text{(III.3)}$$

where E is the C.M. energy. The solution of (3) is facilitated by the decomposition

$$T = \sum_i \tau_{pi}(\epsilon)\,\eta_i(\epsilon) \qquad \text{(III.4)}$$

with

$$\tau_{pi} = V_{pi} + V_{pi}\frac{1}{E-(H-V)+i\varepsilon}\tau_{pi} \qquad \text{(III.5)}$$

Substituting (4) into (3) gives

$$\eta_i(E) = 1 + \frac{1}{E-(H-V)+i\varepsilon}\sum_{j\neq i}^{A}\tau_{pj}\,\eta_j(E) \qquad \text{(III.6)}$$

The set of equations (4)-(6) constitutes the basis of the multiple scattering series which results in the following

$$T = \sum_i \tau_{pi}(E) + \sum_{\substack{i \\ j \neq i}} \tau_{pi}(E) \frac{1}{E - (H-V) + i\epsilon} \tau_{pj}(E)$$

$$+ \text{- - - - -} \qquad \text{(III.7)}$$

At this point it is important to emphasize that τ_{pi} are not two-body projectile-nucleon transition matrices; the propagator $\frac{1}{E - (H-V) + i\epsilon} \equiv G_0(E)$ contains the full nuclear Hamiltonian H_N (see Eq.(1)) and consequently τ_i is a (A+1)-body operator.

The usual procedure is to replace τ_{pi} by the corresponding nucleon-nucleon T-matrix in free space

$$t_{pi}(E) = v_{pi} + v_{pi} \frac{1}{E + \frac{\hbar^2 \nabla^2}{2m} + i\epsilon} t_{pi}(E) \qquad \text{(III.8)}$$

The corrections to the replacement $\tau \to t$ resides in corrections to the free Green function (the replacement of an (A+1) operator by a two-body operator, and to the use of the C.M. energy of the p+1 system in the p-N system (which is reasonable if $A^{-1} \ll 1$).

The stage is now set for the obtention of the optical potential operator which is formally defined by the equation

$$T = v + v \left[P_0 / \left(E + \frac{\hbar^2 \nabla^2}{2m} - K_A \right) \right] T \qquad \text{(III.9)}$$

where $P_0 \equiv |\psi_0\rangle\langle\psi_0|$, is the projection operator onto the target

nucleus ground state, and K_A represents the kinetic energy of the C.M. of the nucleus. Then

$$v = T(E) - T(E) g_0(E) T(E) + \text{- - - .}$$

$$= \sum_i^A t_i(E) + \sum_{i \neq j}^A t_i(E) \frac{1 - P_0}{E + \frac{\hbar^2}{2m}\nabla^2 - K_A} t_j(E)$$

$$+ \text{- - - - - - .} \qquad \text{(III.10)}$$

The ground state state matrix element of V gives us the optical potential for elastic scattering, vis

$$v(E) = \langle \vec{k}', n', 0 | v | \vec{k}, 0, 0 \rangle$$

$$= (2\pi)^3 \delta(\vec{k}' + \vec{n}' - \vec{k}) \, v(\vec{k}', \vec{k}, E) \qquad \text{(III.11)}$$

where $\vec{n}'$ is the center-of mass momentum of the target nucleus, and $\vec{k}$ is the momentum of the projectile. The first order potential obtained from Eq. (III.10) reads

$$v^{(1)}(\vec{k}', \vec{k}; E) = A \int \frac{d\vec{p}_1}{(2\pi)^3} \phi_0(p_1 + \vec{q}; \vec{p}_1) t(\vec{k}_1', \vec{k}_1; E')$$

(III.12)

where ϕ_0 is the target nucleus density matrix, which is related to the density by

$$\rho(\vec{q}) = \int \frac{d\vec{p}_1}{(2\pi)^3} \phi_0(\vec{p}_1 + \vec{q}; \vec{p}_1) \qquad \text{(III.13)}$$

$$\vec{q} = \vec{k}' - \vec{k} \quad , \quad \vec{k}_1 = \vec{k} - \frac{\mu}{m}\left(\vec{k} + \vec{p}_1\right) \qquad \text{and}$$

$$\vec{k}_1' = \vec{k}' - \frac{\mu}{m}\left(\vec{k}' + \vec{p}_1\right)$$

$$E' = E - \left(\vec{k} + \vec{p}_1\right)^2 / 2\left(m_p + m\right)$$

The next step is to set $\vec{p}_1 = 0$ in t, which results in the "tρ" expression

$$v^{(1)}(\vec{k}', \vec{k}; E) = A\, \rho(q)\, t\left(\vec{k}_1', \vec{k}_1; E\right)$$

$$\approx A\, \rho(q)\, t\left(\theta = 0°; E\right) \qquad \text{(III.14)}$$

The last form ignores off-shell effects. It has the advantage of supplying a model indpendent procedure for discussing nucleon-nucleus elastic scattering. The reactive content of $V^{(1)}$, as is known, is quasi-free knock-out[13]. It is to be expected that the impulse approximation form of $V^{(1)}$, Eq. (III.14) would be valid at intermediate proton energies ($E_p \geq 200$ MeV). At these energies, the nucleon-nucleon scattering is practically purely elastic (except for very small bremsstrahlung emission). At higher energies, pion production becomes important ($E_{pN}^{C.M.} \simeq 130$ MeV). This is clearly seen from Fig. (1), showing the total reaction cross section for the free nucleon-nucleon system. Clearly medium effects modify this picture to some extent (e.g. shifting

the pion production threshold to lower energies). Further, these same nuclear medium effect like Pauli blocking and Fermi motion of the target nucleus, bring about changes in the form of $V^{(1)}$ (validity of impulse approximation) as well as make higher order corrections, related to nucleon-nucleon correlations, more important.

Among the numerous corrections required for a better treatment of the scattering process, the second order, double-scattering, effect seems to be the easiest to estimate.

This term looks like, in momentum space (using the free nucleon-nucleon t-matrix as basic input)[25]

$$\langle \vec{k}', 0 | V^{(2)} | \vec{k}, 0 \rangle = \sum_{i=1}^{A} \sum_{j \neq 1} \sum_{\alpha} \int \frac{d\vec{k}''}{(2\pi)^3} \langle \vec{k}', 0 | t_i | \vec{k}'', \alpha \rangle \cdot \frac{1}{E - \frac{\vec{k}''^2}{2m} - E_\alpha + i\varepsilon} \langle \vec{k}'', \alpha | t_j | \vec{k}, 0 \rangle$$

(III.15)

Several approximations are usually employed to simplify the above. Use an average nuclear exctiation energy in the free Green function, $E_\alpha \to \bar{E}_\alpha \equiv \bar{E}$, employ closure to get rid of the $\sum_{\alpha \neq 0} \equiv \sum_{\alpha} - |0\rangle\langle 0|$, and employ the eikonal (high energy approximation) in evaluating the Green's function. Introducing the two particle correlation function

$$\rho^{(2)}(\vec{r}',\vec{r}) = \frac{1}{A(A-1)} \int \psi_0^{\dagger}(\vec{r}_1,\ldots\vec{r}_A) \sum_{i=1}^{A} \sum_{j\neq i} \delta(\vec{r}-\vec{r}_i)\,\delta(\vec{r}'-\vec{r}_j) \cdot \psi_0(r_1,\ldots\vec{r}_A)\, d\vec{r}_1 \cdots\cdots d\vec{r}_A \qquad \text{(III.16)}$$

one can then write an approximate form for the double scattering contribution, which in coordinate space looks like

$$V^{(2)}(r) \simeq -\frac{ik}{2E}\left(V^{(1)}(r)\right)^2 R_{corr.} \qquad \text{(III.17)}$$

where $V^{(1)}$ is the first-order "tρ" potential and $R_{corr.}$ is the two-particle correlation length, given by

$$R_{corr.} = \int_0^{\infty} \left[\frac{\rho^{(2)}(\vec{r}',\vec{r})}{\rho(r')\,\rho(r)} - 1\right]_{(\vec{r}-\vec{r}')} d(r-r') \qquad \text{(III.18)}$$

where a further assumption on the quantity $\rho^{(1)}/\rho\rho$ has been made, namely that it depends only on the relative separation between the two nucleons and not on their individual positions. In the absence of two-body correlations, $R_{corr.} = 0$. In general, it is expected that $\rho^{(2)}(\vec{r}',r)$ would approach the

no-correlation form at separations larger than of the hard core radius (~ 0.4 fm). At smaller separations $\rho^{(2)} = 0$. Thus $R_{corr.} = -0.4$ fm.

The estimate given above for $R_{corr.}$ is very crude. A more refined, treatment of $R_{corr.}$ presented by Ray[26] that it is actually composed of four distinct contributions

$$R_{corr} = R_{Pauli} + R_{SRD} + R_{PSR} + R_{c.m.} \qquad \text{(III.19)}$$

where, following Boridy and Fesbach[27] R_{PAULI} is related to the Pauli exclusion principle correlations, R_{SRD} is related to the short range dynamical correlations and R_{PSR} is connected to a combination of Pauli and short-range dynamic term. Finally $R_{C.M.}$ arises from center of mass correlations. We give below the approximate expressions for these four contributions to $R_{corr.}$ derived by Ray[26]

$$-R_{PAULI} = \frac{1}{2}\left[1 - \frac{5}{A} + \frac{4}{A^2}\right]\frac{3\pi}{10\,k_F(r)}\,\frac{1}{1+\frac{8}{5}\bar{B}\,k_F^2(r)}$$

$$-R_{SRD} = \frac{1}{2}\left[1 - \frac{2}{A} + \frac{1}{A^2}\right]\sqrt{\pi}\,\frac{b^3}{b^2+8\bar{B}} \qquad \text{(III.20)}$$

$$R_{PSR} = \frac{1}{2}\left[1 - \frac{5}{A} + \frac{4}{A^2}\right]\frac{3\pi}{10}\,\frac{1}{\left(k_F^2(r)+\frac{5}{b^2}\right)^{1/2}} \times \left[1 + 8\bar{B}\left(\frac{k_F^2(r)}{5} + \frac{1}{b^2}\right)\right]^{-1}$$

$$-R_{c.m.} = \left(1 - \frac{2}{A} + \frac{1}{A^2}\right) l_c$$

where the parameters A, $k_F(r)$, $\bar{B}$, b, ℓ_c are the target mass number, local Fermi momentum, finite range parameter of nucleon-nucleon elastic t-matrix, short-range dynamical correlation parameter and the effective "correlation length", rexpectively. We should mention that $\bar{B}$ exhibits a non-negligible energy dependence: 0.66 at $E_{LAB} = 100$ MeV and dropping to about 0.1 at $E_{LAB} = 2200$ MeV.

We have evaluated $R_{corr.}$, according to Eqs. (III.19) and (III.20) for the system $p + {}^{12}C$ at several proton laboratory energies. The results are presented in Fig. (5). As can be seen in this figure the dominant contributions to $R_{corr.}$ arise from the Pauli and center of mass correlations. Further, the values of the calculated $R_{corr.}$ over a wide range of proton energies approximates closely the very simple estimate for $R_{corr.}$ given earlier, namely -0.411 fm.

We see clearly from our approximate form for $V^{(2)}$ Eq. (III.17) that the multiple scattering series is an expansion in order of correlation. The third and high order terms, would depend on three and many body correlations. No simple expressions is found for these terms. In the next sub-section we shall employ the above theoretical developments for the calculation of the ion-ion interaction at intermediate energies.

III-2. NUCLEUS-NUCLEUS "$t\rho_1\rho_2$" INTERACTION

Once the nucleon-nucleus potential operator is constructed, the corresponding nucleus-nucleus potential can in principle, be obtained, with due care to antisymmetrization by a folding procedure. In discussing heavy ion reactions at low energies, it has been customary to employ the double folding prescription in conjunction with an effective nucleon-nucleon interaction (G-matrix) which contains most of the nuclear medium effects. A more thorough discussion of this has been given by Satchler and Love, who write for the ion-ion real potential the following

$$Re\, V = \int d\vec{r}_1 \int d\vec{r}_2\, \rho_1(\vec{r}_1)\, \rho_2(\vec{r}_2)\, v(\vec{r}_{12} = \vec{R} + \vec{r}_2 - \vec{r}_1) \qquad \text{(III.21)}$$

where v is given by the M3y

$$v(\vec{r}_{12}) = 6315 \frac{e^{-4r_{12}}}{4r_{12}} - 1961 \frac{e^{-2.5r_{12}}}{2.5\, r_{12}} + J_{oo}\, \delta(\vec{r}_{12})$$

with

$$J_{oo} = -891 \ \ Mev\ fm^3$$

The last term in the above expression for v takes into account the nucleon exchange effects. No energy dependence is present in the above expression. Of course at higher energies, above

should be replaced by the more appropriate nucleon-nucleon G - or t-matrix, which, when inserted in the double folding integral above, would determine the energy dependence of the resulting, complex ion-ion potential. Thus, following the discussion of the previous section we write

$$\mathcal{V}^{(1)}_{A_1 A_2}(r) \cong t(\theta=0;E)\int d\vec{r}\,'\,\rho_{A_1}(\vec{r})\,\rho_{A_2}(\vec{r}-\vec{r}\,')$$

$$= -4\pi\frac{E}{k^2} f_{NN}(\theta=0;E)\int d\vec{r}\,'\,\rho_{A_1}(\vec{r}\,')\,\rho_{A_2}(\vec{r}-\vec{r}\,') \qquad \text{(III.22)}$$

where f_{NN} is the nucleon-nucleon scattering amplitude. With the help of the optical theorem, we may now obtain the imaginary part of $\mathcal{V}^{(1)}_{A_1 A_2}(r)$

$$-\mathrm{Im}\,\mathcal{V}^{(1)}_{A_1 A_2}(r) = -\frac{E}{k}\sigma_{NN}(E)\int \rho_{A_1}(\vec{r}\,')\,\rho_{A_2}(\vec{r}-\vec{r}\,')\,d\vec{r}\,' \qquad \text{(III.23)}$$

which is clearly just the proton-nucleus imaginary interaction folded onto the projectile density.

The real part of $\mathcal{V}^{(1)}_{A_1 A_2}(r)$, which would correspond to the intermediate energy version of the double folding interaction, can be obtained from the systematics of $\mathrm{Re}\,f_{NN}$. One usually writes[26]

$$\mathrm{Re}\,f_{NN} = \alpha\,\mathrm{Im}\,f_{NN} \qquad \text{(III.24)}$$
$$\mathrm{Im}\,f^{NN}_{N\lambda} = (k\,\sigma^{T}_{NN}/4\pi)\exp[-a_{NN}q^2]$$

The parameter α depends on the nucleon energy, attaining the value of 0.06 at $E_{LAB} = 800$ and becoming negative at E > 1000 MeV. In table I we present the values of the physical parameters that determine f_{NN} at several Lab. energies. As a consequence of Eq. (III.24) and table I, the real part of $\mathcal{V}^{(1)}_{A_1 A_2}$ at E/N ≈ ≈ 1000 should become attractive. We turn now to the consideration of the second-order (double scattering) contribution to the ion-ion potential.

Our recipe for this contribution is to perform a symmetrized single folding with the projectile and target densities. This then suggests

$$\mathcal{V}^{(2)}_{A_1 A_2}(r) = -\frac{ik}{4E}\mathcal{R}_{corr}\left\{\int\left[\mathcal{V}_{NA_1}(\vec{r}-\vec{r}\,')\right]^2\rho_{A_2}(\vec{r}\,')\,d\vec{r}\,' + \int\left[\mathcal{V}_{NA_2}(\vec{r}-\vec{r}\,')\right]^2\rho_{A_1}(\vec{r}\,')\,d\vec{r}\,'\right\} \qquad \text{(III.25)}$$

where $\mathcal{V}^{(1)}_{NA_1}(r)$ is the nucleon-nucleus (A_1) "tp" type optical potential discussed earlier.

We have evaluated the second order (double scattering)

correction to the "$t\rho_1\rho_2$" potential, according to Eq. (III.25), with $R_{corr.}$ given by Eqs. (III.19), (III.20) for the system $^{12}C + ^{12}C$ at the following Lab. energy per nucleon 100, 200, 300 and 500 MeV. In Figures 6 and 7, we show the radial distributions of the second order correction to the optical potential for the $^{12}C + ^{12}C$ system at the above energies. For comparison, we also show the contribution of the dominant, "$t\rho_1\rho_2$", DF, potential at 100 MeV/N. The range of the second-order potential is appreciably shorter than that of the first one owing to the high-order density dependence; "$(t\rho_1)^2\rho_2$" vs. "$(t\rho_1)\rho_2$"[29]. It is interesting to note that the imaginary part of optical potential changes at 100 MeV/N namely, $W^{(2)}$ is regenerative whereas at the other cited energies it is absorptive. We should stress, though, that the summed contributions of $W^{(1)}$ and $W^{(2)}$ is guaranteed to be absorptive. The above behaviour of $W^{(2)}$ is a consequence of the folding formula (III.25). Using explicitly the form of $\mathcal{V}^{(1)}$ Eq. (III.20), we have

$$Re\, \mathcal{V}^{(2)} = -\frac{E}{2k}|R_{corr}| \propto \sigma_T^2 \langle \rho_{A_1}^2 \rho_{A_2} + \rho_{A_2}^2 \rho_{A_1} \rangle (r)$$

$$Im\, \mathcal{V}^{(2)} = \frac{E}{4k}|R_{corr}|(\alpha^2-1)\sigma_T^2 \langle \rho_{A_1}^2 \rho_{A_2} + \rho_{A_2}^2 \rho_{A_1} \rangle (r) \qquad \text{(III.26)}$$

$$\langle \rho_{A_1}^2 \rho_{A_2} + \rho_{A_2}^2 \rho_{A_1} \rangle (r) \equiv \int \rho_{A_1}^2 (r-r') \rho_{A_2}(r')\, dr' + \int \rho_{A_2}^2 (r-r') \rho_{A_1}(r')\, dr' \qquad \text{(III.27)}$$

Therefore $Re\, \mathcal{V}^{(2)}$ being linear in Ref_{NN} (and correspondingly in the parameter α) is attractive in the energy range $100 < E < 800$ MeV and repulsive at $E_{LAB} > 1000$ MeV. In contrast $Im\, \mathcal{V}^{(2)}$ behaves as (α^2-1) and thus is regenerative at those energies where $\alpha > 1$ and absorptive at the other energies where $\alpha < 0$. The sum $Im\, \mathcal{V}^{(1)} + Im\, \mathcal{V}^{(2)}$ is guaranteed to be always negative (absorptive) as unitarity requires.

In our calculation of the ion-ion optical potential to be described later, we have used Pauli-blocking corrected nucleon-nucleon total cross sections. The full details of the structure of $Im\,(\mathcal{V}^{(1)} + \mathcal{V}^{(2)})$, which is used later for the calculation of σ_R, are given in the following section. Here we may mention that owing to the fact that the volume integral of $\mathcal{V}^{(2)}$ is 0.3 of that of $\mathcal{V}^{(1)}$, it is expected that the effect of $\mathcal{V}^{(2)}$ on σ_R is small. We have verified this by evaluating, within the JWKB approximation discussed in Section II, the total reaction cross section of $^{12}C + ^{12}C$ using $\mathcal{V}^{(1)} + \mathcal{V}^{(2)}$ for an optical potential and have found that $\mathcal{V}^{(2)}$ has a less than 10% influence on σ_R with respect to the calculation with only $\mathcal{V}^{(1)}$ included. In our calculation, to be described fully in Section IV, we have included the Pauli-blocking effect mentioned above, and performed an appropriate average over the Fermi motion of the nucleons in the projectile and target.

IV. THE IMAGINARY PART OF THE "$t\rho_1\rho_2$" INTERACTION

In this Section we develop further the theory of the imaginary part of the ion-ion potential discussed in the previous Section. In particular we investigate the effect of Pauli blocking on the potential and the consequent effect on the mean free path. Other medium effects such as the binding energy, off-shell effects and the non-locality of the potential will also be briefly discussed.

As we have seen in the previous Section, the imaginary part of the "$t\rho_A\rho_B$" interaction, can be written in the following form

$$W(E;\vec{r}) = -\frac{E}{k_N}\sigma_T^{NN}(E)\int d\vec{r}'\,\rho_A(\vec{r}-\vec{r}')\,\rho_B(\vec{r}') \qquad \text{(IV.1)}$$

where E and k_N are the energy and momentum per nucleon, respectively, and σ_{NN}^T is the nucleon-nucleon total cross section. The Pauli blocking is included in the above expression for W, by modifying (reducing) σ_{NN}^T. According to Kikuchi and Kawai[30] this entails substituting σ_{NN}^T above by an average cross section given by, (for the case of proton-nucleus scattering)

$$\overline{\sigma_T^{NN}(E)} = \frac{1}{k_1\frac{4\pi}{3}k_F^3}\int d\vec{k}_2\int d\Omega'\,2k\,\sigma_{NN}(\vec{k},\vec{k}') \qquad \text{(IV.2)}$$

where it is assumed that k_1 is the momentum of the projectile nucleon, k_F is the Fermi momentum of the target, $\vec{k}_2$ is the momentum of a target nucleon, $d\Omega'$ is the element of solid angle that defines the direction of the final relative momentum $\vec{k}'$; $\vec{k}$ is the initial relative momentum and $\sigma_{NN}(\vec{k},\vec{k}')$ is the differential NN cross section. The integrals appearing in Eq. (IV.2) take into account the Pauli blocking through the restriction imposed on $|k_2| < k_F$ and on $d\Omega'$. Assuming an isotropic angular distribution $\sigma(\vec{k},\vec{k}') = \frac{1}{4\pi}\sigma_{NN}^T(k)$, one is then able to derive for $\overline{\sigma}_{NN}^T$, the following simple expression[31]

$$\overline{\sigma_T^{NN}}(E) = \sigma_T^{NN}(E_1)\;P\left(\frac{E_F}{E_1}\right) \qquad \text{(IV.3)}$$

with

$$P(x) = \begin{cases} 1-\frac{7}{5}x & , \quad x \le \frac{1}{2} \\ 1-\frac{7}{5}x+\frac{2}{5}x(2-x^{-1})^{5/2} & , \quad x \ge \frac{1}{2} \end{cases} \qquad \text{(IV.4)}$$

In obtaining Eq. (IV. 3), it is assumed that the free nucleon-nucleon total cross section is independent of energy, which is a reasonable assumption at energies above 100 MeV. Assuming an energy dependence which is proportional to the inverse of the energy, $P(x)$ attains the following form $P(x) \simeq 1-\frac{8}{5}x$

For the nucleus-nucleus interaction, Eq. (IV.1), the incorporation of the Pauli blocking effect into σ_{NN}^{T} is more involved since both projectile and target nucleons are Pauli blocked. No simple expressions for P(x) is obtained in this case and only through numerical integrations is one able to obtain $\bar{\sigma}_{NN}^{T}$. The pertinent formulae as well as the details of the calculation are given in Appendix IV.

The above consideration of Pauli blocking is made in nuclear matter. In actual finite nuclei, we invoke two straightforward modifications on the results obtained so far: the local density approximation, which renders k_F dependent on the radial distance, through $k_F(\rho(r))$,

$$k_F = \left(\frac{3}{2}\pi^2 \rho(r)\right)^{1/3} \qquad \text{(IV.5)}$$

and secondly, we use an average nucleon-nucleon cross section. For nucleon- nucleus scattering we have

$$\langle \bar{\sigma}_T^{NN} \rangle = \left[(A-Z)\,\bar{\sigma}_{Nn} + Z\,\bar{\sigma}_{Np}\right]/A \qquad \text{(IV.6)}$$

where N refers to n or p according to whether the incident nucleon is proton or neutron, respectively. In the absence of Pauli blocking, one expects from Eq. (IV.6) that generally $\langle \sigma_{pN}^{T} \rangle$ is larger than the free p-p or n-n cross section. Of course for N=Z nuclei,

$$\langle \bar{\sigma}_T^{NN} \rangle = \frac{1}{2}\left(\bar{\sigma}_T^{Nn} + \bar{\sigma}_T^{Np}\right)$$
$$= \frac{1}{2}\left(\sigma_T^{Nn} + \sigma_T^{Np}\right) P\left(\frac{E_F}{E}\right) \qquad \text{(IV.7)}$$

the symmetrized σ_T^{NN} relevant for nucleon-nucleus scattering has the form

$$\langle \bar{\sigma}_T^{NN} \rangle = \frac{Z_1 Z_2 + (A_1 - Z_1)(A_2 - Z_2)}{A_1 A_2}\,\sigma_T^{nn} + \frac{Z_1(A_2 - Z_2) + Z_2(A_1 - Z_1)}{A_1 A_2}\,\sigma_T^{np}$$

Since within the local-density approximation $\bar{\sigma}_{NN}$ and $\langle \bar{\sigma}_{NN} \rangle$ are r-dependent, the expression for W , Eq. (IV.1), becomes

$$W(E;r) = -\frac{E}{k_N}\int d\vec{r}'\, \rho_A(\vec{r}-\vec{r}')\,\rho_B(\vec{r}') \cdot \langle \bar{\sigma}_{NN} \rangle \left(E, k_F^A(r,r'), k_F^B(r')\right) \qquad \text{(IV.8)}$$

To take a better account of the surface, we have also corrected $k_F(r)$ to become[32]

$$k_F^{i\,2}(r) = \left(\frac{3}{2}\pi^2 \rho_i(r)\right)^{2/3} + \frac{5}{2}\left(\frac{\vec{\nabla}\rho_i}{\rho_i}\right)^2 \qquad \text{(IV.9)}$$

where ξ is of the order of 0.1 . The above form of k_F is the one employed in the calculation of W Eq. (IV.8). The Fermi momentum of each nucleus has been determined using Eq. (IV.9) by dividing the space occupied by the nucleus into three regions, internal, central and surface.

Using the above as well as the results of Appendix IV we have calculated the Pauli blocking modified N-N cross sections. In figures (8 and 9) we present the behaviour of $\bar{\sigma}_{PP}$ and $\bar{\sigma}_{NP}$ vs. k . Also shown are the free space cross sections. Different values of the Fermi momentum of the target nucleus, $k_{F,1}$, $k_{F,2}$, were used for the purpose of comparison. In figures (10) and (11) are shown the effective $\bar{\sigma}$,s appropriate for nucleus-nucleus scattering, for different values of the Fermi momenta $k_{F,1}$ and $K_{F,2}$ of the two ions.

From these figures, one can see clearly that the Pauli blocking reduction in the values of the $\bar{\sigma}$,s is greater in the nucleus-nucleus systems than that in the nucleon-nucleus systems at higher energies. At lower energies the situation is inverted quite drastically. In fact at $k < k_F$, the effective nucleon-nucleon cross sections in the nucleon-nucleus case approaches zero. On the other hand, at these low energies the nucleus-nucleus $\bar{\sigma}_{NP}$ and $\bar{\sigma}_{PP}$ is non-negligible. This is so due to the increased rôle of the surface nucleons that still have enough energy owing to Fermi motion which enables them to

scatter nucleons into the Pauli-allowed angular region.

It is commonly assumed that the total nucleon-nucleon cross section in free space is slowly varying function of energy and is consequently replaced by a constant. Such a procedure is used, e.g. to derive the Pauli-modified cross section, Eq. (IV.3). However, in the energy region of interest to us, the energy dependence of the free cross sections is quite strong and has to be taken into account, as we have done here.

We are now in a position to calculate W. In figure (12) and (13) we present our results for two systems. Also shown is the W evaluated with the free σ_{NN}^{T} , for comparison. Clearly Pauli blocking reduces greatly the strength of W at lower energies as expected. At intermediate and high energies the Pauli blocking effect is reduced in importance, and W approaches the one with free σ_{NN}^{T} . We should mention that at low energies, other reactions mechanisms besides single nucleon knockout come into play rendering our calculated W with Pauli blocking certainly smaller than the W extracted from adjustment of the total reaction cross section. This we discuss fully in the next Section. To take into account the effect of these other mechanisms, one has to have a model for W which accounts for the excitation of collective surface excitation, as well as for fusion.

V. CALCULATION OF σ_R FOR SEVERAL HEAVY ION SYSTEMS

Having obtained the microscopic ion-ion potential in the previous Sections, we are now in a position to test it in so far as its reactive content is concerned. Further, the range of dominance in W of inclusive single-nucleon knockout at intermediate energies can now be assessed. In this Section we present a detailed account of our calculation of the total reaction cross section, σ_R, for several heavy-ion systems. In particular we discuss the degree of transparancy in these systems and how this is related to the mean free path, as discussed qualitatively in Section II. Another related question which is addressed here is the dependence of σ_R on the effective radius of the system and how this dependence changes with energy. In our calculation, we also include the second-order double NN scattering potential discussed in Section III.

The expression we use for σ_R is the WKB one given in Eqs. (II.13), (II.17) and (II.21), namely

$$\sigma_R = 2\pi \int b\,db\, [1 - \exp(-4\delta_I(b))] \qquad (V.1)$$

with $\delta_I(b)$ given by Eq. (II.19), and evaluated for the $t\rho_1\rho_2$ potential discussed in the Section III, with the Pauli blocking effects fully incorporated as done in Section IV.

The expression we use for σ_R contains the effect of refraction arising from the real part of the heavy ion interaction potential [3]. It also contains an improvement over the treatments of other authors in that we include, besides the usual nuclear medium corrections, the second-order double scattering component discussed in Section III.

We have calculated σ_R for several heavy-ion systems, ranging from light, such as the very extensively studied $^{12}C + ^{12}C$, to the very heavy $^{208}Pb + ^{208}Pb$. Our aim in this, is not so much the reproduction of the existing data, but rather to pin down the energy region in which the "tρρ" interaction approximates well the complex ion-ion potential, with its reactive content being predominantly single- and double-nucleon knockout (single knockout and double knockout being respectively associated with the imaginary parts of the single scattering "$t\rho_1\rho_2$" and double scattering "$(t\rho_1)^2\rho_2$" interactions). As we shall see, at low energies, where Pauli blocking greatly reduces the strength of the imaginary part, as we have seen in the previous Section, the calculated total reaction cross section, according to Eq. (V.1) becomes much smaller than the data, as it should, since no account is taken of nuclear surface inelastic excitation, fusion and other processes which dominate σ_R at these energies.

In Figure (14) we present the result for $^{12}C + ^{12}C$. The full curve represents the result obtained with Eq. (V.1), including the Coulomb and the real part of the nuclear potentials.

In the energy range $100 < E_{C.M.} < 800$ MeV/A the agreement with the data is reasonable. At lower energies, however, our calculation underestimates the data by a factor which could be as large as 2 at $E_{C.M.} \sim 10$ MeV/A. The dashed curve represent the result without V_N and V_C and with no Pauli blocking. The fact that this curve approximates very well the data is clearly fortuituous. The crosses shown represent the result of nuclear matter calculation reported by Faessler et al. [4]. This calculation seems to come close to our calculation when Pauli blocking is taken into account, but with no V_N and V_C (shown as dashed-dotted line). It is important to notice that both Pauli blocking and nuclear + Coulomb refractive effects are quite insignificant at higher energies. Thus it is in the low energy regime that the theory gets its major check. Of course it is exactly at these energies, where other nuclear processes, not accounted for by the "tρρ" interaction, start coming into play, as already discussed. These processes gradually fill in the gap between the calculated microscopic σ_R and the data. Of these, incomplete fusion and deep inelastic processes, are probably the most important at $5 < E < 15$ MeV/A, followed by complete fusion. Inelastic and transfer reactions as well as other quasi-elastic processes always contribute with varying weights, depending on energy.

We have also calculated σ_R for other systems. In Figs. (15)-(22), we show our result for, $^{12}C + ^{40}Ca$, $^{40}Ca + ^{40}Ca$, $^{12}C + ^{90}Zr$, $^{90}Zr + ^{90}Zr$, $^{12}C + ^{208}Pb$, $^{40}Ca + ^{208}Pb$, $^{90}Zr + ^{208}Pb$, and $^{208}Pb + ^{208}Pb$. These systems were chosen to represent different mass regions. In some cases few data points exist, in others, none. In all cases, we see the clear drop in σ_R (full curves) as the energy is lowered, indicating the approach to the threshold of the processes described by the "$t\rho_1\rho_2$" interaction. Further, the small dip in σ_R close to the effective threshold for single pion production in the nucleon-nucleon scattering becomes less conspicuous as the mass of the heavy ion system increases.

Having calculated microscopically the total reaction cross section from the "$t\rho_1\rho_2$" interaction, it is now possible to evaluate the degree of transparancy in the different HI systems at intermediate energies. Before doing this, it is useful to establish first the connection between our calculated results for σ_R and the geometrical formula given by Eq. (II.16)

$$\sigma_R = \pi R^2 \left(1 - \frac{V_B}{E_{c.m.}}\right) \qquad (V.2)$$

We have considered the following systems $^{12}C + ^{208}Pb$, $^{40}Ca + ^{208}Pb$, $^{90}Zr + ^{208}Pb$ and $^{208}Pb + ^{208}Pb$ at $\frac{E_{C.M.}}{A}$: 10, 200, 400 and 600 MeV. To reproduce the theoretical values of σ_R with Eq. (V.2), we were forced to use the following small values of the radius parameter r_o ($R = r_o(A_1^{1/3} + A_2^{1/3})$), 1,22, 1,26, 1,26, and 1,26 fm respectively, for the four systems mentioned above.

These values for r_o are considerably smaller than what one might expect if the geometrical limit of σ_R has been reached by these systems. Such limit is usually specified by the strong absorption radius which gives for $r_o \simeq 1{,}5$ fm. In fact to reproduce the available $^{12}C + ^{12}C$ data, shown in Fig. (14) at $\frac{E_{C.M.}}{A} \simeq 5$ MeV, we need to use $r_o = 1.57$ fm. It is therefore clear that these systems do exhibit a large degree of transparancy T (Eq. (II.27)) as was suggested by several authors. However, one has to be careful when assessing this transparancy since there is a strong dependence on the value of r_o used. For example according to Bohlen et al.[9b] there is a 12% transparancy in $^{12}C + ^{12}C$ at $\frac{E_{C.M.}}{A} \simeq 12$ MeV whereas De Vries et al.[2] predict a zero value for T. Such a discrepancy stems from the fact that these authors use different values for the strong absorption radius parameter in Eq. (V.2).

We present now our calculation of T, based on our theoretical results, which we compare to the following equation

$$\sigma_R = \pi R_B^2 \left(1 - \frac{V_B}{E_{c.m.}}\right)(1 - T) \qquad (V.3)$$

with a radius parameter r_o, of about 1.5. For the $^{12}C + ^{12}C$ system this parameter is slightly larger ($r_o = 1.57$). In Table (II) we show our results for $^{12}C + ^{12}C$, $^{12}C + ^{208}Pb$, $^{40}Ca + ^{40}Ca$ and $^{208}Pb + ^{208}Pb$ at $\frac{E_{C.M.}}{A} = 50$, 100, 200, 300 and 500 MeV.

We see clearly that the transparancy factor ranges in value from about 50% for the lightest system to about 27% for the heaviest one.

In our calculation of σ_R presented so far, we did not take into account the effect of statistics in the identical projectile target systems. We now discuss this point, and present estimates of the effect.

The elastic scattering amplitude $f(\theta)$ should be written as

$$\overline{f(\theta)} = f(\theta) + \tau (-)^{2I-S} f(\pi - \theta) \qquad (V.4)$$

where $\tau = +(-)$ for boson (fermions), and I is the intrinsic spin of the partners and s denotes the channel spin $s = 0,1,2,\ldots.2I$. In what follows we take the case of two bosons with I=0 (e.g. ^{12}C). Thus, through the application of the optical theorem to $\overline{f}(\theta)$, and with $P_\ell(\theta) = (-)^\ell P_\ell(\pi-\theta)$, we obtain

$$\overline{\sigma}_R = \frac{\pi}{k^2} \sum_{\ell=0}^{\infty} (2\ell+1)\left[1 + (-)^\ell\right] T_\ell \qquad (V.5)$$

which can be written, in the impact parameter representation, as

$$\overline{\sigma}_R(E) = 2\pi \int_0^\infty db\, b \left[1 + \cos(kb - \tfrac{1}{2})\right] T(b) \qquad (V.6)$$

where we have used $(-1)^{\ell} = \cos\pi\ell$ and $\ell + \frac{1}{2} = kb$.

Let us now evaluate the above expression in the sharp cut off model, namely

$$T(b) = \Theta(b_c - b) \tag{V.7}$$

where b_c is the Coulomb modified sharp cut off radius. Then

$$\overline{\sigma_R}(E) = \sigma_R(E) + \Delta\sigma_{stat.} \,, \tag{V.8}$$

$$\sigma_R(E) = \pi b_c^2 \tag{V.9}$$

$$\Delta\sigma_{stat.} = 2\pi \left\{ \frac{b_c}{\pi} \sin(k b_c - 1/2) + \frac{1}{k^2}\left[\cos(k b_c - 1/2) - \cos(1/2)\right] \right\} \tag{V.10}$$

In the above expression $\Delta\sigma_{stat}$ represents the correction to σ_R arising from the identity of the particles.

In table I we present the values of $\Delta\sigma_{stat}$ for several identical heavy ion systems at several C.M. energies per nucleon. We see clearly that $\Delta\sigma_{stat}$ contributes at most about 5% at these energies. At higher energies the effect is even smaller. Thus, for all practical purposes, we can ignore $\Delta\sigma_{stat}$. The use of the more realistic T(b), in Eq. (V-1) does not change appreciably the above conclusions.

VI. CONCLUSIONS

It is quite obvious from our results presented in the previous Chapters, that the "$t\rho_1\rho_2$"-interaction, corrected for by Pauli blocking and higher-order multiple scattering effects, is only adequate for accounting the absorptive content of the HI interaction, in a limited energy domain, contrary to several recent claims [2]. This energy region is dominated by single and/or double nucleon knockout processes. At lower energies the Pauli blocking, though slightly weakened by the attractive nuclear interaction, reduces significantly the contributions of these processes to the total reaction cross section. This is also the conclusion reached when a nuclear matter, G-matrix calculation is performed [4].

To account for σ_R at $\frac{E}{A} < \epsilon_F$, several channels, related principally to mean field effects, such as fusion, incomplete fusion, deep inelastic, nuclear quasi-elastic and particle transfer channels, have to be added to the knockout channel. This has been partially made by Faessler [4]. More work is clearly needed.

APPENDIX I - DERIVATION OF σ_R FROM THE WRONSKIAN

In this Appendix, we supply a derivation of σ_R using explicitly the optical Schrodinger equation

$$-\frac{\hbar^2}{2\mu}\nabla^2\psi^{(+)}+(V-iW)\psi^{(+)}=E\psi^{(+)} \qquad (A.I.1)$$

where we take $W>0$ to describe absorption. From (A.I.1) one can immediately derive the equation for flux conservation,

$$\hbar\int\vec{\nabla}\cdot\vec{J}\,d^3r=2\langle\psi^{(+)}|W|\psi^{(+)}\rangle \qquad (A.I.2)$$

where $\vec{J}$ in the probability current

$$\vec{J}=\frac{\hbar}{2\mu i}\left[\psi^*\vec{\nabla}\psi-(\vec{\nabla}\psi^*)\psi\right] \qquad (A.I.3)$$

Applying Gauss' theorem to the LHS of (A.I.2), we have then

$$-\int\vec{J}\cdot d\vec{A}=\frac{2}{\hbar}\langle\psi^{(+)}|W|\psi^{(+)}\rangle \qquad (A.I.4)$$

where the integral is over any surface surrounding the interaction, in a region where the potential has vanished. Eq. (A.I.4) simply says that the net radial flux is not zero because of absorption. The total reaction cross section is defined as the net inward radial flux given by the LHS of (A.I.4) devided by

the incident flux $|\psi^{(+)}|^2 v$, where v is the asymptotic relative velocity

$$\sigma_R=\frac{-\int\vec{J}\cdot d\vec{A}}{|\psi^{(+)}|^2 v}=\frac{2}{\hbar v}\,\frac{\langle\psi^{(+)}|W|\psi^{(+)}\rangle}{|\psi^{(+)}|^2} \qquad (A.I.5)$$

If we choose the normalization of $\psi^{(+)}$ to be $|\psi^{(+)}|^2=1$ we obtain our expression for σ_R Eq. (II.9)

$$\sigma_R=\frac{2}{\hbar v}\langle\psi^{(+)}|W|\psi^{(+)}\rangle=\frac{k}{E}\langle\psi^{(+)}|W|\psi^{(+)}\rangle \qquad (A.I.6)$$

We leave it to the reader to convince himself that Eq. (A.I.4) can be written in the more familiar optical theorem form,

$$\frac{4\pi}{k}\,Im f(0)-\int|f(\theta)|^2 d\Omega=\frac{k}{E}\langle\psi^{(+)}|W|\psi^{(+)}\rangle \qquad (A.I.7)$$

where the first term is the total cross section and the second the total elastic cross section. Clearly (A.I.6) is consistent with (A.I.7).

The extention of the above considerations to coupled channels is straightforward. Instead of Eq. (A.I.1) we now have to consider the following

$$-\frac{\hbar^2}{2\mu}\nabla^2\psi_0^{(+)}+(V_0-iW_0)\psi_0^{(+)}=E\psi_0^{(+)}-\sum_{j\neq 0}V_{0j}\cdot\psi_j^{(+)} \qquad (A.I.8)$$

where W_0 represents the absorptive potential in $|\psi_0^{(+)}\rangle$, in the limit $V_{oj} = 0$.

Gauss' theorem then gives

$$-\int \vec{j}\cdot d\vec{A} = \frac{2}{\hbar}\langle\psi_o^{(+)}|W|\psi_o^{(+)}\rangle + \frac{2}{\hbar}\,\mathrm{Im}\langle\psi_o^{(+)}|V_{oj}G_j^{(+)}V_{jo}|\psi_o^{(+)}\rangle \qquad \text{(A.I.9)}$$

The second term on the left hand side represents the contribution to $\int \vec{j}.d\vec{A}$ arising from the channels j, coupled to the entrance channel. This term can be further decomposed, as was shown in Chapter II, into a genuine open channels contribution and closed channels contributions (fusion). In fact, taking V_{oj} to be Hermitian, we have[19]

$$\begin{aligned}
&\mathrm{Im}\langle\psi_o^{(+)}|V_{oj}G_j^{(+)}V_{jo}|\psi_o^{(+)}\rangle = \langle\psi_o^{(+)}|V_{oj}\,\mathrm{Im}\,G_j^{(+)}V_{jo}|\psi_o^{(+)}\rangle \\
&= \sum_j \langle\psi_o^{(+)}|V_{oj}\left(-\pi|\psi_j^{(-)}\rangle\langle\psi_j^{(-)}|\right)V_{jo}|\psi_o^{(+)}\rangle \\
&- \langle\psi_o^{(+)}|V_{oj}G_j^{(+)\dagger}W_jG_j^{(+)}V_{jo}|\psi_o^{(+)}\rangle \\
&= -\pi\int|\langle\psi_j^{(-)}|V_{jo}|\psi_o^{(+)}\rangle|^2\,d\Omega_j \\
&- \sum_j \langle\psi_j^{(+)}|W_j|\psi_j^{(+)}\rangle
\end{aligned} \qquad \text{(A.I.10)}$$

Accordingly, (A.I.6) becomes now

$$\sigma_R = \frac{k}{E}\left[\langle\psi_o^{(+)}|W_o|\psi_o^{(+)}\rangle + \sum_{j\neq o}\langle\psi_j^{(+)}|W_j|\psi_j^{(+)}\rangle\right] + \sigma_D \qquad \text{(A.I.11)}$$

where σ_D describes the direct channels contribution.

APPENDIX II - COMPARISON BETWEEN $\delta_I^{(WKB)}$ AND $\delta_I^{(Eikonal)}$

In this short Appendix we present a comparison between the imaginary part of the nuclear elastic phase shift calculated within the eikonal approximation, Eq. (II.22),

$$\delta_I^{(E)}(b) = -\frac{1}{4}\frac{2\mu}{\hbar^2 k}\int_{-\infty}^{\infty} dz\, W\left(\sqrt{b^2+z^2}\right) \qquad (A.II.1)$$

with the more precise one obtained within the WKB approximation, Eq. (II.19)

$$\delta_I = \frac{2\mu}{\hbar^2}\int_{r_1}^{\infty} dr' \left[\left(E - \frac{Eb^2}{r'^2} - U(r')\right)^2 + W^2(r')\right]^{1/4} \sin\frac{\theta(r')}{2} \qquad (A.II.2)$$

$$\tan\theta(r') = \frac{-W(r')}{\left(E - \frac{Eb^2}{r'^2} - U(r')\right)}$$

for several cases, involving the $^{12}C+^{12}C$ system, using $U(r')=0$ for simplicity. A Woods-Saxon form was employed for $W(r')$

$$W(r) = \frac{-W_0}{1+\exp\left(\frac{r-R_0}{a}\right)} \qquad (A.II.3)$$

with $a = 0.6$ fm and $R_0 = 8.0$ fm. W_0 was varied.

The results are presented in figure (23). Clearly

the higher energy is the better agreement one obtains between the two expressions. In the applications described in this paper, we have always employed the WKB expression with the real part of the potential taken into account.

APPENDIX III - RELATIVISTIC, DIRAC, FORM OF THE TOTAL REACTION CROSS SECTION

The discussion and calculation of σ_R presented in this paper was based on non-relativistic scattering theory. In recent years, it has become quite clear that proton-nucleus scattering at intermediate energies is more correctly described by a relativistic Dirac optical equation. In particular, spin polarization and rotation seem quite clearly to require, for their description, such a relativistic theory. One would also like to check whether such a relativistic theory will influence σ_R. In this Appendix, we present the relativistic formulation of σ_R and apply it to proton-nuclear scattering[23].

The Dirac equation that describe the elastic scattering of a nucleon, treated as a Dirac particle, from a spin-saturated nucleus, is usually written in the form, using a time-independent description.

$$\left[\vec{\alpha}\cdot\vec{p} + \beta\left(m+V_s\right) + V_o\right]\psi = E\psi \qquad \text{(A.III.1)}$$

where it is assumed that the average, complex, nucleon-nucleus potential is a sum of a scalar component, V_s, and the fourth (time) component of a vector potential, V_o. The matrices $\vec{\alpha}$ and β are Dirac's, and ψ is the four-component vector wave-function.

Let us write V_s and V_o as

$$V_s = U_s - i W_s$$
$$V_o = U_o - i W_o \qquad \text{(A.III.2)}$$

Eq. (A.III.1) can be rewritten as

$$\left[\gamma_4(E-V_o) - i\vec{\gamma}\cdot\vec{p} - (m+V_s)\right]\psi = 0 \qquad \text{(A.III.3)}$$

obtained from the usual relations, $i\vec{\gamma} \equiv \gamma_4\vec{\alpha}$, $\gamma_4 \equiv \beta$. We now perform the usual manipulations of multiplying Eq. (A.III.3) from the left by $\bar{\psi} = \psi^\dagger\gamma_4$ and constructing its conjugate with the subsequent multiplication from the left by ψ, to obtain finally

$$\bar{\psi}\left[(\gamma_4(E-V_o) - i\vec{\gamma}\cdot\vec{p} - (m+V_s)\right]\psi = 0 \qquad \text{(A.III.4)}$$
$$\bar{\psi}\left[(\gamma_4(E-V_o^\dagger) - i\vec{\gamma}\cdot\vec{p} - (m+V_s^\dagger)\right]\psi = 0 \qquad \text{(A.III.5)}$$

the usual Wronskian argument used in Appendix I now supplies us the continuity equation

$$-\vec{\nabla}\cdot\vec{j} = \frac{2}{\hbar}\left(\psi^\dagger W_o\psi + \psi^\dagger\gamma_4 W_s\psi\right) \qquad \text{(A.III.6)}$$

with

$$\vec{j} = i\bar{\psi}\vec{\gamma}\psi \qquad \text{(A.III.7)}$$

the hadronic current.

Integrating Eq. (A.III.6) over a large volume and using Gauss's theorem, gives us

$$-\int_S \vec{J}\cdot d\vec{A} = \frac{2}{\hbar}\langle \psi^{(+)} | (W_0 + \gamma_4 W_s) | \psi^{(+)} \rangle \qquad \text{(A.III.8)}$$

where the integral is over a surface surrounding the potential, in a region where the potential has completely vanished, and describes the net inward flux due to absorption ($W_0 \neq 0$, $W_s \neq 0$). Dividing this flux by the incident current $\frac{v}{(1-(v/c)^2)^{\frac{1}{2}}} \equiv v\gamma$ (assuming that $\psi^{(+)}$ in normalized to unity), gives the total reaction cross section

$$\sigma_R = \frac{-\int_{s\to\infty}\vec{J}\cdot d\vec{A}}{v\gamma} = \frac{2}{\hbar v\gamma}\langle \psi^{(+)} | W_0 + \gamma_4 W_s | \psi^{(+)} \rangle \qquad \text{(A.III.9)}$$

We remind the reader again that $\psi^{(+)}$ is a scattering vector wave function.

Eq. (A.III.9) can be further reduced to a form more convenient for numerical evaluation. We do this by explicitly writing $\psi^{(+)}$ in terms of its upper (large) and lower (small) components,

$$\psi^{(+)} = \left(\frac{E+m}{2m}\right)^{1/2} \begin{pmatrix} 1 \\ \frac{1}{A}\vec{\sigma}\cdot\vec{p} \end{pmatrix} u_s \qquad \text{(A.III.10)}$$

where

$A = E + m + V_s - V_0$, and u_s satisfies the reduced Dirac equation

$$\left(\vec{\sigma}\cdot\vec{p}\,\frac{1}{A}\,\vec{\sigma}\cdot\vec{p} - E - m - V_s - V_0\right) u_s = 0 \qquad \text{(A.III.11)}$$

with Eq. (A.III.10), σ_R, Eq. (A.III.9), becomes

$$\sigma_R = \frac{E+m}{\hbar v\gamma m}\left[\int d^3r\,(W_0+W_s)\,u_s^\dagger u_s + -(W_s-W_0)\left(\frac{1}{A}\vec{\sigma}\cdot\vec{p}\,u_s\right)^\dagger\left(\frac{1}{A}\vec{\sigma}\cdot\vec{p}\,u_s\right)\right] \qquad \text{(A.III.12)}$$

Using the fact that $(W_s-W_0)/|A|^2 = \frac{1}{2i}(A^{-1}-A^{\dagger-1})$, we can, after performing one integration by parts and using Gauss' theorem on the second term on the RHS of Eq. (A.III.12), write for σ_R the following surface integral

$$\sigma_R = -\frac{1+\gamma}{2v\gamma}\int_S dA\left[u_s^\dagger\left(\frac{\vec{\sigma}\cdot\hat{n}}{A}\,\vec{\sigma}\cdot\vec{p}\,u_s\right) + +\left(\frac{\vec{\sigma}\cdot\hat{n}}{A}\,\vec{\sigma}\cdot\vec{p}\,u_s\right)^\dagger u_s\right] \qquad \text{(A.III.13)}$$

which reduces, in the appropriate $s\to\infty$ limit, where $A\to E+m = (1+\gamma)m$, to the final expression

$$\sigma_R = -\frac{1}{mv\gamma}\int_{S\to\infty} dA\ Re\left(u_s^\dagger\,\vec{\sigma}\cdot\hat{n}\,\vec{\sigma}\cdot\vec{p}\,u_s\right) \qquad (A.III.14)$$

Eq. (A.III.14) could have been obtained directly from the first part of Eq. (A.III.9) namely from the identification $\sigma_R = \frac{-1}{\gamma v}\int_{S\to\infty} d\vec{A}\cdot\vec{j}$. Our derivation above serves as a check of the correctness of Eq. (A.III.9). In the following, we evaluate Eq. (A.III.14) in the eikonal (small-angle) limit.

The eikonal approximation to $\psi^{(+)}$ or u_s of Eq. (A.III.1) or (A.III.11), has been recently discussed by Amado et al.[35]. Here we derive an eikonal form for σ_R, starting with Eq. (A.III.14). We follow the notation of Ref. (35).

Within the eikonal approximation to u_s, we have, as $r\to\infty$

$$\vec{p}\,u_s \xrightarrow[r\to\infty]{} mv\gamma\,\hat{z}\,u_s \qquad (A.III.15)$$

Using Eq. (A.III.15) in Eq. (A.III.14), we obtain

$$\sigma_R = -\int_{S\to\infty} dA\ u_s^\dagger\,\hat{n}\cdot\hat{z}\,u_s \qquad (A.III.16)$$

Since S is any large surface surrounding the interaction potential, we may take for it two planes perpendicular to the z-axis at $z = \pm\infty$. We thus have

$$\sigma_R = \int d^2b\left[|u_s|^2(\vec{b},z\to-\infty) - |u_s|^2(\vec{b},z\to+\infty)\right] \qquad (A.III.17)$$

Eq. (A.III.17) exhibits very nicely the physical meaning of in terms of the probability densities $|u_s|^2(\vec{b},z\to-\infty)$ and $|u_s|^2(\vec{b},z\to+\infty)$.

Using the usual substitution for the upper component

$$u^{(+)}_{\vec{k},s} = e^{i\vec{k}\cdot\vec{r}}\,e^{iS(\vec{r})}\,\chi_s \qquad (A.III.18)$$

where χ_s are Dirac spinors and $S(\vec{r})$ satisfies the differential equation

$$\vec{k}\cdot\vec{\nabla}S(\vec{r}) = -m\left\{V_c(r) + V_{so}(r)\left[\vec{\sigma}\cdot\vec{r}\times\vec{k} - i\,\vec{n}\cdot\vec{k}\right]\right\} \qquad (A.III.19)$$

In Eq. (A.III.19) the central, $V_c(r)$ and spin-orbit, V_{so} interaction are given by (see Eq. (A.III.11))

$$V_c(r) = V_s(r) + \frac{E}{m}V_o(r) + \frac{V_s^2(r) - V_o^2(r)}{2m} \qquad (A.III.20)$$

$$V_{so}(r) = \frac{1}{2mA}\,\frac{1}{r}\,\frac{d}{dr}\left(V_o(r) - V_s(r)\right) \qquad (A.III.21)$$

and $\vec{k} = \frac{1}{2}(\vec{k}+\vec{k}')$, the average of the initial and final momenta.

Defining the z-axis to be along the direction of $\vec{k}$, the eikonal phase $S(\vec{r})$, can be written as

$$i\,S(\vec{r}) = -\frac{m}{k}\int_{-\infty}^{z} dz'\left\{V_c(b,z') + V_{so}(\vec{b},z')\left[\vec{\sigma}\cdot\vec{b}\times\vec{k} - ikz'\right]\right\} \quad \text{(A.III.22)}$$

Using Eq. (A.III.22) in Eq. (A.III.18), we can write down immediately for $|u_s|^2(\vec{b},z)$ the following

$$|u_s|^2(\vec{b},z) = \chi_s^{\dagger}\exp\left[-2\,\mathrm{Im}\,S(\vec{b},z)\right]\chi_s \quad \text{(A.III.23)}$$

We remind the reader that S is an operator in spin space.

Let us introduce the quantities

$$F = E - V_0(\vec{b},z) \quad \text{(A.III.24)}$$

$$N = m - V_s(\vec{b},z) \quad \text{(A.III.25)}$$

Then Eqs. (A.III.17), (A.III.20) and (A.III.21) give us for

$$\sigma_R = \chi_s^{\dagger}\left[\int d^2b\,\left(1 - e^{\phi(b)}\right)\right]\chi_s \quad \text{(A.III.26)}$$

where

$$\phi(\vec{b}) = \phi_c(\vec{b}) - \phi_{so}(\vec{b})\,\vec{\sigma}\cdot(\hat{b}\times\hat{k}) \quad \text{(A.III.27)}$$

and

$$\phi_c(\vec{b}) = \frac{1}{(\hbar c)^2 k}\int_{-\infty}^{\infty} dz\ \mathrm{Im}\,(N^2 - F^2) \quad \text{(A.III.28)}$$

$$\phi_{so}(\vec{b}) = b\int_{-\infty}^{\infty} dz\,\frac{1}{r}\,\mathrm{Im}\left[\frac{1}{F+N}\frac{\partial}{\partial r}(F+N)\right] \quad \text{(A.III.29)}$$

At this point it is worth mentioning that the quantities $\phi_c(\vec{b})$ and $\phi_{so}(\vec{b})$, are related to the thickness functions, $t_c(\vec{b})$ and $t_{so}(\vec{b})$ of Amado et al.[35], defined by

$$t_c(b) = \frac{-i}{2(\hbar c)^2 k}\int_{-\infty}^{\infty} dz'\left(N^2 - F^2 + E^2 - m^2\right) \quad \text{(A.III.30)}$$

$$t_{so}(b) = \frac{-ib}{2}\int_{-\infty}^{\infty} dz'\,\frac{1}{F+N}\,\frac{1}{r}\frac{\partial}{\partial r}(F+N) \quad \text{(A.III.31)}$$

Thus

$$\phi_c(b) = 2\,\mathrm{Re}\;t_c(b) \quad \text{(A.III.32)}$$

$$\phi_{so}(b) = 2\,\mathrm{Re}\;t_{so}(b) \quad \text{(A.III.33)}$$

Going back to Eq. (A.III.26), we note first that we can write it as

$$\sigma_R = \chi_s^{\dagger}\left[\int d^2b\,\left(1 - e^{\phi_c(b)}\,e^{-\phi_{so}(b)\,\vec{\sigma}\cdot\hat{b}\times\hat{k}}\right)\right]\chi_s$$

$$= \chi_s^+ \Big[\int d^2b \Big(1 - e^{\Phi_c(b)} \cosh \Phi_{so}(b) + \vec{\sigma} \cdot (\hat{b} \times \hat{k}) e^{\Phi_c(b)} \cdot \sinh \Phi_{so}(b) \Big] \chi_s$$

$$= 2\pi \chi_s^+ \Big[\int b db \Big(1 - e^{\Phi_c(b)} \cosh \Phi_{so}(b) \Big) \Big] \chi_s$$

$$= 2\pi \int_0^\infty b db \Big(1 - e^{\Phi_c(b)} \cosh \Phi_{so}(b) \Big) \qquad \text{(A.III.34)}$$

The term involving $\vec{\sigma} \cdot \hat{b} \times \hat{k}$ does not contribute to the b-integral due to symmetry about the z-axis, Eq. (A.III.34) can also be written as (Eqs. (A.III.32) and (A.III.33))

$$\sigma_R = 2\pi \int_0^\infty b db \Big(1 - e^{2Re\, t_c(b)} \cosh 2Re\, t_{so}(b) \Big) \qquad \text{(A.III.35)}$$

Eq. (A.III.35) is the principal result of this section. It expresses σ_R in the usual form of an impact parameter integral involving "relativistic" transmission coefficients given by

$$T(b) = 1 - e^{2Re\, t_c(b)} \cosh 2Re\, t_{so}(b) \qquad \text{(A.III.36)}$$

It is clear that the exact form and details of T(b) would be irrelevant if the nucleon-nucleus scattering is dominated by a black disk-type absorption. In such a case T(b) would be representable as

$$T(b) = \Theta(b - R_c) \qquad \text{(A.III.37)}$$

where $\Theta(x)$ is the step function, and R_c is a characteristic absorption radius. If Eq. (A.III.37), is used σ_R becomes the simple geometrical limit,

$$\sigma_R = \pi R_c^2 \qquad \text{(A.III.38)}$$

If the above were true, not too much physics would be extracted from σ_R. Luckily total reaction cross section data of proton-nucleus systems at intemediate energies exhibit major deviations from the black disk result Eq. (A.III.38). Nuclei become quite transparent to nucleons at intermediate energies[2], and the quantity that measures this nuclear transparency in details is given by T(b) of Eq. (A.III.36). Therefore detailed evaluation and discussion of T(b) and the resulting σ_R is clearly called for. This has been done using the conventional non-relativistic theory by Digiacomo, De Vries and Peng[2]. In the following we present our result for and discussion of σ_R within the Dirac-eikonal treatment presented in this section.

Before presenting our results, we warn the reader that $t_c(b)$ is ill-defined for proton scattering because of the presence of the long range Coulomb potential which is present in $V_o(r)$. This difficulty can be dealt with easily by some

appropriate modification of the integral involved. The details are given in Appendix I of Ref.23). Here we only cite the final Coulomb-modified, but finite, σ_R

$$\sigma_R = 2\pi \int_0^\infty b\,db \left(1 - e^{2Re\tilde{t}_c(b)} \cosh 2\,Re\, t_{s_0}(b)\right) \qquad \text{(A.III.39)}$$

$$\tilde{t}_c(b) = \frac{-i}{2(\hbar c)^2 k} \int_{-\infty}^{\infty} dz \left(N^2 + F^2 + E^2 - m^2 - \frac{2E z_1 z_2 e^2}{r(b,z)}\right) \qquad \text{(A.III.40)}$$

Finally, a word about the optical theorem and its generalized version for charged particle scattering. For neutral particles the usual form of the optical theorem

$$\sigma_R = \frac{4\pi}{k} Im\, F(\vec{k},\vec{k};E) - \int |F(\vec{k},\vec{k}';E)|^2 \, d\Omega_{\hat{k}'} \qquad \text{(A.III.41)}$$

should yield the correct expression for σ_R. In fact, with the elastic scattering amplitude $F(\vec{k},\vec{k}';E)$ derived by Amado et al[35,36].

$$F(\vec{k},\vec{k}';E) = F_1 + \vec{\sigma}\cdot\hat{n}\, F_2 \qquad \text{(A.III.42)}$$

$$F_1 = -ik \int_0^\infty db\, b\, J_0(qb) \left(e^{\tilde{t}_c(b)} \cosh t_{s_0}(b) - 1\right) \qquad \text{(A.III.43)}$$

$$F_2 = -k \int_0^\infty db\, b\, J_1(qb)\, e^{\tilde{t}_c(b)} \sinh t_{s_0}(b) \qquad \text{(A.III.44)}$$

$\vec{q} \equiv |\vec{k}-\vec{k}'|$, and J_0 and J_1, are ordinary Bessel functions, Eq. (A.III.41) results in exactly the expression for σ_R given in Eq. (A.III.35).

For charged particle scattering, Eq. (A.III.41) yields infinite values for both terms on the RHS. However, a generalized optical theorem can be derived for the purpose and it does supply a means of calculating σ_R,

$$\sigma_R = \frac{4\pi}{k} Im\left[F(\vec{k},\vec{k};E) - F_c(\vec{k},\vec{k};E)\right] - \int \left[|F_c(\vec{k},\vec{k}';E)|^2 - |F(\vec{k},\vec{k}';E)|^2\right] d\Omega \qquad \text{(A.III.45)}$$

where F_C is the point Coulomb scattering amplitude. In a way, the procedure we employ amounts to basically calculating the difference $F-F_C$ in the form of an impact-parameter integral, which yields completely convergent results.

NUMERICAL RESULTS

In what follows we present the results of our calculation of σ_R, Eq. (A.III.39), for $p + {}^{40}Ca$ and $p + {}^{208}Pb$, in the proton energy range $10 < E_p < 1000$ MeV. We take for the proton-nucleus optical potential, the impulse-approximation Dirac optical interaction for spin-saturated nuclei, has the general form[34]

$$\langle \vec{k}' | U_{oo} | \vec{k} \rangle = -\frac{4\pi i k}{m}\left[F_s(q)\rho_s(q) + \gamma_4 F_V(q)\rho_V(q)\right]$$
$$\equiv V_s(q) + V_o(q) \qquad \text{(A.III.46)}$$

In Eq. (A.III.46), F_S and F_V are the scalar and vector pieces of the Lorentz-invariant N-N amplitude, respectively, and ρ_S and ρ_V are the scalar and vector form factors of the target nucleus, given by

$$\rho_s(q) = \langle o | \sum_i e^{i\vec{q}\cdot\vec{r}_i} | o \rangle \qquad \text{(A.III.47)}$$

$$\rho_V(q) = \langle o | \sum_i \gamma_4^i e^{i\vec{q}\cdot\vec{r}_i} | o \rangle \qquad \text{(A.III.48)}$$

The above densities can be better visualized when written in configuration space,

$$\rho_s(r) = \langle o | \sum_i \gamma_4^i \delta(\vec{r}-\vec{r}_i) | o \rangle \equiv \sum_\alpha^{occ.} \bar{\psi}_\alpha(r)\psi_\alpha(r) \qquad \text{(A.III.49)}$$

$$\rho_V(r) = \langle o | \sum_i \delta(\vec{r}-\vec{r}_i) | o \rangle \equiv \sum_\alpha^{occ.} \psi_\alpha^\dagger(r)\psi_\alpha(r) \qquad \text{(A.III.50)}$$

where we find α-sums are over occupied single particle states. Writing in terms of its upper and lower components,

$$\psi_\alpha = \begin{pmatrix} \psi_\alpha^U \\ \psi_\alpha^L \end{pmatrix}, \quad \bar{\psi} = \left(\psi_\alpha^{U*}, -\psi_\alpha^{L*}\right) \qquad \text{(A.III.51)}$$

we can express $\rho_S(r)$ and $\rho_V(r)$ as

$$\rho_s(r) = \sum_\alpha^{occ.} |\psi_\alpha^U(r)|^2 - \sum_\alpha^{occ.} |\psi_\alpha^L(r)|^2 \equiv \rho_U(r) - \rho_L(r) \qquad \text{(A.III.52)}$$

$$\rho_V(r) = \sum_\alpha^{occ.} |\psi_\alpha^U(r)|^2 + \sum_\alpha^{occ.} |\psi_\alpha^L(r)|^2 \equiv \rho_U(r) + \rho_L(r) \qquad \text{(A.III.53)}$$

Therefore, the difference $\rho_V(r) - \rho_S(r)$, measures the strength of the lower component density $2\rho_L(r)$, and accordingly, the degree to which the optical potential is relativistic.

The potential calculated by McNeil et al.[34], is obtained by setting $F_S(q) \approx F_S(0)$ and $F_V(q) \approx F_V(0)$ in Eq. (A.III.46). In this limit, which is quite reasonable in the energy range considered, the Fourier transform of Eq. (A.III.46) yields a local potential in configuration space, with its γ-dependence completely specified by $\rho_S(r)$ and $\rho_V(r)$. We therefore write

$$V_s(r) = V_s^o(E)\hat{\rho}_S(r) = \left(U_s^o(E) - iW_s^o(E)\right)\hat{\rho}_S(r) \qquad \text{(A.III.54)}$$

$$V_o(r) = V_o^o(E)\hat{\rho}_V(r) = \left(U_o^o(E) - iW_o^o(E)\right)\hat{\rho}_V(r) \qquad \text{(A.III.55)}$$

where $\hat{\rho}_S$ and $\hat{\rho}_V$ represent the shape of the densities and

they are both normalized to unity in the central region. McNeil et al.[34] presented their results for $U_S^o(E)$. $W_S^o(E)$. $U_o^o(E)$ and $W_o^o(E)$ at a radius where ρ_S and ρ_V are both 0.16 fm^{-3}. These values of the densities, correspond to a Fermi momentum, $k_F = 1.37\ fm^{-1}$. It is found that W_S^o is negative, implying, using our convention, Eq. (A.III.2), that the scalar interaction is regenerative whereas the vector one is absorptive. Their values come out comparable, with $W_o^o(E)$ a bit larger than W_S^o. All of these results are in accord with phenomenological findings. The above results were also confirmed by Horowitz[38] in his nuclear matter calculation of W_S and W_o.

Armed with the above facts, we evaluated σ_R, Eq. (A.III.39), using the results of McNeil et al., as presented in their figure 1. For the density shape of ^{208}Pb we have used Saxon-Wood forms with parameters fixed in accordance with results obtained from electron scattering, which basically supplies ρ_V for portons. We have, however set $\hat{\rho}_S(r) = \hat{\rho}_V(r)$ for all r. The radius, R, and diffuseness, a, parameters for ^{208}Pb, are [2]

$$R = 6.624\ fm \quad , \quad a = 0.549\ fm$$

The density shape of ^{40}Ca is usually parametrized as

$$\hat{\rho}_{Ca^{40}}(r) = \left(1 + \omega r^2/R^2\right) \Big/ \left[1 + \exp\left(r - R\right)/a\right] \qquad (A.III.56)$$

with $\omega = -0.1017$, $R = 3.669$ fm, $a = 0.584$ fm.

The results are presented in Figures 24 and 25. It is clear from the figures that the comparison of our σ_R in the energy range $100 < E < 1000$ MeV, with the data[2], is as good as the one obtained with the nonrelativistiv theory. This finding convinces us that our calculation of σ_R for heavy-ions presented in this paper, with the conventional nonrelativistic "$t\rho_1\rho_2$" potential should be adequate.

APPENDIX IV - PAULI BLOCKING EFFECTS ON THE NUCLEUS-NUCLEUS TOTAL CROSS SECTION

1. CALCULATION OF $\bar{\sigma}_{NN}(E)$ FOR NUCLEON-NUCLEUS SCATTERING

In the first part of this Appendix, we review the calculation of $\bar{\sigma}_{NN}$ in nucleon-nucleus scattering. Although this has been discussed extensively by several authors, we feel that a full review is necessary as a preparation for the calculation of $\bar{\sigma}_{NN}$ in the nucleus-nucleus case, presented in the second part of this Appendix.

The average cross section of two nucleons, one of which is found with momentum k_2 is given by

$$\bar{\sigma} = \frac{1}{V_{F_2}} \int_{V_{F_2}} d\vec{k}_2 \, \sigma_T^{NN}(\vec{q},\vec{q}') \qquad \text{(A.IV.1)}$$

where $V_{F_2} \equiv \frac{4}{3}\pi k_{F_2}^3$ is the volume of the Fermi sphere representing the target nucleus (labeled here by 2), and $\sigma_T^{NN}(\vec{q},\vec{q}')$ is the free nucleon-nucleon cross section, which depends on the relative momenta $\vec{q} = \vec{k}_1 - \vec{k}_2$ and $\vec{q}' = \vec{k}_1' - \vec{k}_2'$, before and after the collision, respectively, where $\vec{k}_1$ is the incident nucleon momentum. When using Eq.(A.IV.1) one normally employs for σ_T^{NN} an empirical form, which is valid for fixed target nucleons. To correct for this, namely for the fact that $\vec{k}_2 \neq 0$, one inserts a transformation factor, $\frac{|\vec{k}_1 - \vec{k}_2|}{k_1}$, giving thus

$$\bar{\sigma} = \frac{1}{V_{F_2}} \int d\vec{k}_2 \, \frac{|\vec{k}_1 - \vec{k}_2|}{k_1} \, \sigma_T^{NN} \qquad \text{(A.IV.2)}$$

Clearly, Pauli blocking enters through the restriction, $|\vec{k}_1'| > k_{F_2}$, $|\vec{k}_2'| > k_{F_2}$, or $\vec{k}_1'^2 + \vec{k}_2'^2 > 2k_F^2$. Therefore, when expressed in terms of the differential cross section, Eq. (A.IV.2) takes the form, in the energy region where $\sigma^T = \int d\Omega \frac{d\sigma}{d\Omega}$,

$$\bar{\sigma} = \frac{1}{V_{F_2}} \int d\vec{k}_2 \, \frac{|\vec{k}_1 - \vec{k}_2|}{k_1} \int_{|\vec{k}_1' + \vec{k}_2'|^2 > 2k_{F_2}^2} d\Omega \, \frac{d\sigma}{d\Omega} \qquad \text{(A.IV.3)}$$

Using now energy and momentum conservation, we can recast the above equation into the following form

$$\bar{\sigma}_\lambda = \frac{1}{V_{F_2}} \int d\vec{k}_2 \, \frac{|\vec{k}_1 - \vec{k}_2|}{k_1} \int_{k_1'^2 + k_2'^2 > 2k_{F_2}^2} d\Omega \, \delta(\vec{q} - \vec{q}') \, d\vec{q}' \, \frac{d\sigma}{d\Omega} \qquad \text{(A.IV.4)}$$

$(k_1'^2 + k_2'^2 = k_1^2 + k_2^2)$

After integrating over q' and , we obtain, assuming $\frac{d\sigma}{d\Omega} = \frac{\sigma_{NN}^T(q)}{4\pi}$, the following

$$\bar{\sigma} = \frac{1}{k_1 V_{F_2}} \int d\vec{k}_2 \, \frac{|k_2^2 + k_1^2 - 2k_{F_2}^2|}{|\vec{k}_1 + \vec{k}_2|} \, \sigma_{NN}^T(q) \qquad \text{(A.IV.5)}$$

where the lower limit of integration, obeys, $k_1^2 + k_2^2 > 2k_{F_2}$.

It is a usual practice to assume that $\sigma_{NN}^{T}(q)$ is a constant, σ_0, which results in the following simple expression for $\bar{\sigma}_{NN}$

$$\bar{\sigma}_{NN} = \begin{cases} \sigma_0 \left[1 - \frac{7}{5}\left(\frac{k_{F_2}^2}{k_1^2}\right)\right] & k_1^2 \geq 2k_{F_2}^2 \\ \sigma_0\left[1 - \frac{7}{5}\left(\frac{k_{F_2}^2}{k_1^2}\right) + \frac{2}{5}\frac{k_{F_2}^2}{k_1^2}\left(2 - \frac{k_1^2}{k_{F_2}^2}\right)^{5/2}\right], & k_1^2 \leq 2k_{F_2}^2 \end{cases} \qquad \text{(A.IV.6)}$$

which are nothing but Eqs. (IV.3, IV.4), mentioned in Section IV.

In the application we envisage in this paper, we shall use the empirical energy-dependent $\sigma_{NN}^{T}(q)$. For this purpose, a more convenient form for the evaluation of $\bar{\sigma}_{NN}$ is the following, equivalent, relation

$$\bar{\sigma}_{NN} = \frac{1}{k_1 V_{F_2}} \int d\vec{k}_2 \, |\vec{k}_1 - \vec{k}_2| \, \frac{\sigma_{NN}^{T}(q)}{4\pi} \int_{Pauli} d\Omega \qquad \text{(A.IV.7)}$$

where the restrictions imposed by the conservation laws and Pauli's principle are contained implicitly in the solid angle integral. The above form of $\bar{\sigma}_{NN}$ is the one which is most easily adaptable to the ion-ion case.

In the calculation of the integral $\int_{Pauli} d\Omega$, one resorts to geometrical arguments. Pauli blocking, within the Fermi gas model used here, implies a restriction on the lengths of the

vectors $\vec{k}_1'$ and $\vec{k}_2'$, as visualized in figure (26a). The momenta $\vec{k}_1$ and $\vec{k}_2$ define the total momentum $2\vec{p} = \vec{k}_1 + \vec{k}_2$ and the relative momentum $2\vec{q} = \vec{k}_1 - \vec{k}_2$, with $\vec{p}$ specifying the center of the scattering sphere and $\vec{q}$ its radius, as indicated in figure (26b), the conservation of linear momentum implies fixed $\vec{p}$. From energy conservation, we also have $\vec{k}_1 \cdot \vec{k}_2 = \vec{k}_1' \cdot \vec{k}_2'$ and $\vec{q} = \vec{q}'$, which implies a constant radius for the scattering sphere. Imposing now Pauli blocking, gives

$$\begin{aligned} |\vec{k}_1'| &= |\vec{p} + \vec{q}'| > k_{F_2} \\ |\vec{k}_2'| &= |\vec{p} - \vec{q}'| > k_{F_2} \end{aligned} \qquad \text{(A.IV.8)}$$

which implies that the amount of solid angle not allowed is as indicated in figure (26c) by the dashed area. Thus $\int_{Pauli} d\Omega = 4\pi - \Omega_a$, which when inserted in Eq. (A.IV.7), yields the closed expression, Eq. (A.IV.6), if a constant $\sigma_T^{NN}(q)$ is used. The solid angle portion Ω_a is given by (obtained directly from Eq. (A.IV.8))

$$\Omega_a = 4\pi - \frac{2\pi\,(k_1^2 + k_2^2 - 2k_{F_2}^2)}{2q \cdot 2p} \, . \qquad \text{(A.IV.9)}$$

2. CALCULATION OF $\bar{\sigma}_{NN}(E)$ FOR NUCLEUS-NUCLEUS SCATTERING

In the nucleus-nucleus case, the calculation of $\bar{\sigma}_{NN}(E)$ involves the considerations of three spheres; the two Fermi spheres representing the projectile and target nuclei and the scattering sphere, determined by the momentum and energy conservation laws and the Pauli principle, in close analogy with the considerations presented in the first part of this Appendix.

The starting expression for $\bar{\sigma}_{NN}$ in the nucleus--nucleus case is

$$\overline{\sigma_{NN}}(k, k_{F_1}, k_{F_2}) = \frac{1}{V_{F_1} V_{F_2}} \int d\vec{k}_1\, d\vec{k}_2 \frac{2q}{k} \frac{\sigma_{NN}^{T}(q)}{4\pi} \cdot \int_{Pauli} d\Omega \qquad \text{(A.IV.10)}$$

where $V_{F_1} = \frac{4}{3}\pi k_{F_1}^3$ and $V_{F_2} = \frac{4}{3}\pi k_{F_2}^3$ being the Fermi volume of the projectile and target nuclei, respectively and $2q = |\vec{k}_1 - \vec{k}_2 + \vec{k}|$ with k denoting the relative momentum per nucleon.. In figure (27a) we present the three momentum spheres alluded to above. Using similar arguments as those discussed in the first part of this Appendix, leads us to conclude that the region <u>not</u> allowed by the Pauli exclusion principle in the nucleus-nucleus case, is the one shown as the shaded region in figure (27b).

The restricted solid angle integral is

$$\int_{Pauli} d\Omega = \Omega_{Pauli}(\theta_a, \theta_b, \theta) = 4\pi - 2\Omega_a - 2\Omega_b + \bar{\Omega} \qquad \text{(A.IV.11)}$$

where Ω_a and Ω_b are the solid angles specifying the excluded cones and $\bar{\Omega}$ represents the intersection area of the two conical sections. The solid angles Ω_a and Ω_b are easily determined, as was done earlier

$$\Omega_a = 2\pi(1 - \cos\theta_a)$$
$$\Omega_b = 2\pi(1 - \cos\theta_b) \qquad \text{(A.IV.12)}$$

where

$$\cos\theta_a = \frac{p^2 + q^2 - k_{F_2}^2}{2pq}$$
$$\cos\theta_b = \frac{p^2 + q^2 - k_{F_1}^2}{2bq} \qquad \text{(A.IV.13)}$$

and

$$2\vec{p} = \vec{k}_2 + \vec{k} + \vec{k}_1$$
$$2\vec{q} = \vec{k}_2 - \vec{k} - \vec{k}_1$$
$$\vec{b} = \vec{k} - \vec{P} \qquad \text{(A.IV.14)}$$

The evaluation of $\bar{\Omega}$ is tedious but straightforward[39]. We give below the pertinent expressions. Two possibilities arise

$$1)\quad \bar{\Omega} = 2\Omega_i(\vartheta,\vartheta_a,\vartheta_b) + 2\Omega_i'(\pi-\vartheta,\vartheta_a,\vartheta_b) \quad , \quad \vartheta+\vartheta_a+\vartheta_b > \pi \qquad \text{(A.IV.15)}$$

$$2)\quad \bar{\Omega} = 2\Omega_i(\vartheta,\vartheta_a,\vartheta_b) \quad , \quad \vartheta+\vartheta_a+\vartheta_b \leq \pi \qquad \text{(A.IV.16)}$$

where the angle ϑ is given by

$$\cos\vartheta = \frac{k^2-p^2-b^2}{2pb} \qquad \text{(A.IV.17)}$$

The solid angle Ω_i has the following values,

$$a)\quad \Omega_i = 0 \quad , \quad \vartheta \geq \vartheta_a+\vartheta_b \qquad \text{(A.IV.18)}$$

$$b)\quad \Omega_i = 2\left\{\cos^{-1}\left[\frac{\cos\vartheta_b - \cos\vartheta\cos\vartheta_a}{\sin\vartheta_a\sqrt{\cos^2\vartheta_a+\cos^2\vartheta_b-2\cos\vartheta\cos\vartheta_a\cos\vartheta_b}}\right]\right.$$
$$+\cos^{-1}\left[\frac{\cos\vartheta_a - \cos\vartheta\cos\vartheta_b}{\sin\vartheta_b\sqrt{\cos^2\vartheta_a+\cos^2\vartheta_b-2\cos\vartheta\cos\vartheta_a\cos\vartheta_b}}\right]$$
$$-\cos\vartheta_a\cos^{-1}\left[\frac{\cos\vartheta_b-\cos\vartheta\cos\vartheta_a}{\sin\vartheta\sin\vartheta_a}\right]$$
$$\left.-\cos\vartheta_b\cos^{-1}\left[\frac{\cos\vartheta_a-\cos\vartheta\cos\vartheta_b}{\sin\vartheta\sin\vartheta_b}\right]\right\}$$

$$, \quad |\vartheta_b-\vartheta_a| \leq \vartheta \leq \vartheta_a+\vartheta_b \qquad \text{(A.IV.19)}$$

$$c)\quad \Omega_i = \Omega_b \quad , \quad \vartheta_a \geq \vartheta_b \quad , \quad \vartheta \leq |\vartheta_b-\vartheta_a| \qquad \text{(A.IV.20)}$$

$$d)\quad \Omega_i = \Omega_a \quad , \quad \vartheta_a \leq \vartheta_b \quad , \quad \vartheta \leq |\vartheta_b-\vartheta_a| \qquad \text{(A.IV.21)}$$

The first case above represents the situation where no intersection of the two conic sections, a and b, occur.

We would mention that it may happen in some cases, for several values of p, q and k_{F_1}, the cosine functions above attains unphysical values (> 1). These cases are

$$\begin{aligned} &1)\ p+q < k_{F_2} && , \cos\vartheta_a < -1 \\ &2)\ |p-q| > k_{F_2} && , \cos\vartheta_a > +1 \\ &3)\ b+q < k_{F_1} && , \cos\vartheta_b < -1 \\ &4)\ |b-q| > k_{F_1} && , \cos\vartheta_b > 1 \end{aligned} \qquad \text{(A.IV.22)}$$

Under the conditions 1 and 3 we merely set $\int_{\text{Pauli}} d\Omega$ equal to zero, since the scattering sphere in this case is situated inside the Fermi sphere of either the target or projectile nucleus. If, on the other hand, cos $_a$ > 1 and cos $_b$ > 1 (conditions 2 and 4) then two possilities are considered

$$|p-q| > k_{F_2} \begin{cases} p > q \longrightarrow \Omega_a = 0 \\ p < q \longrightarrow \Omega_{\text{Pauli}_2}(\vartheta_a,\vartheta_b,\vartheta) = 0 \end{cases} \qquad \text{(A.IV.23)}$$

$$|b-q| > k_{F_1} \begin{cases} b > q \longrightarrow \Omega_b = 0 \\ b < q \longrightarrow \Omega_{Pauli}(\theta_a, \theta_b, \theta) = 0 \end{cases} \qquad \text{(A.IV.24)}$$

The cases $\Omega_a = 0$ and Ω_b represent the situation when the scattering sphere does not intersects the Fermi spheres.

In Eq. (A.IV.10) the average nucleon-nucleon cross section $\bar{\sigma}_{NN}$ clearly depends on the Fermi momenta k_{F_1} and k_{F_2} which are related to the matter densities according to [32]

$$k_F^2(r) = \left(\frac{3}{2}\pi^2 \rho(r)\right)^{2/3} + \frac{5}{2}\xi\left(\frac{\vec{\nabla}\rho}{\rho}\right)^2 \qquad \text{(A.IV.25)}$$

where the second term amounts to a surface correction with ξ about 0.1 .

In our calculation of $\bar{\sigma}_{NN}$, we have used the above expression for k_{F_1} and k_{F_2} in Eq. (A.IV.10), which was evaluated numerically. simple analytic expression, such as given in Eq. (IV.3) for the nucleon-nucleus case, was found, even in the limiting case of constant free nucleon-nucleon total cross section.

REFERENCES

1. P.J. Karol - Phys.Rev. C11 (1975) 1203
2. R.M. De Vries and J.C. Peng - Phys.Rev. C22 (1980) 1055; see also N.J. Di Giacomo and R.M. De Vries - Comm.Nucl. Part.Phys. 12 (1984) 111.
3. D.M. Brink and G.R. Satchler - J.Phys.G. 7 (1981) 43.
4. A. Faessler, L. Rikus and S.B. Khadkibar - Nucl.Phys. A401 (1983) 157.
5. J.C. Peng, R.M. De Vries and N.J. Di Giacomo - Phys.Lett. 98B (1981) 244.
6. H.B. Bidasaria, L.W. Townsend and J.W. Wilson - J.Phys.G 9 (1983) L17.
7. M. Buenerd, J. Pinston, J. Cole, C. Guet, D. Lebnen, J.M. Loiseaux, P. Martin, E. Monnand, J. Mougey, H. Nifenecher, R. Ost, P. Perrin, Ch. Ristori, P. de Saintignon, F. Schussler, L. Carlén, H.A. Gustafsson, B. Jakobsson, T. Johansson, G. Jönsson, J. Krumlinde, I. Otterlund, H. Ryde, B. Schröder, G. Tibell, J.B. Bondorf and O.B. Nielsen - Phys.Lett. 102B (1981) 242.
8. A.J. Cole, W.D.M. Rae, M.E. Brandan, A. Dacal, B.G. Harvey, R. Legrain, M.J. Murphy and R.G. Stokstad - Phys. Rev.Lett. 47 (1981) 1705.
9. C. Perrin, S. Kox, N. Longequeue, J.B. Viano, M. Buenerd, R. Cherkaoui, A.J. Cole, A. Gamp, J. Menet, R. Ost, R. Bertholet, C. Guet and J. Pinston - Phys.Rev.Lett. 49 (1982) 1905;

H.G. Bohlen et al. - Z.Phys. A308 (1982) 121.

S. Kox et al. - Phys.Lett. 159B (1985) 15.

10. R.M. De Vries, N.J. Giacomo, J.S. Kapustinsky, J.C. Peng, W.E. Sondheim, J.W. Sunier, J.G. Gramer, R.E. Loveman, C.R. Gruhn and H.H. Wieman - Phys.Rev. C26 (1982) 301.
11. W.O. Lock and D.F. Measday - Intermediate Energy Nuclear Physics (Methuen Co. LTD, 1970).
12. See, e.g., P. Braun-Munzinger et al. - Phys.Rev.Lett. 52 (1984) 255; R. Shyam and J. Knoll in Proc. Workshop on Coinc.Part.Emis. from Contin.States in Nuclei Edit. H. Machner and P. Jahn (World Scientific, 1984) 582.
13. P.C. Tandy, E.F. Redish and O. Bollé - Phys.Rev.Lett. 35 (1975) 921; Phys.Rev. C16 (1977) 1924;
D.S. Koltun and D.M. Schneider - Phys.Rev.Lett. 42 (1979) 211.
14. J.T. Haldemann and R.M. Thaler - Phys.Rev.Lett. 14 (1965) 81; Phys.Rev. 139 (1965) 131186.
15. M.S. Hussein, H.M. Nussenzveig, A.C.C. Villari and J.Cardoso Jr. - Phys.Lett. 114B (1982) 1;
see also A.Z. Schwarzchild, E.H. Auerbach, R.C. Fuller and S. Kahana - Proc.Symp.on Macroscopic Features of Heavy-Ion Collisions - ANL Report ANL-PHY-76-2.
16. H. Bethe - Phys.Rev. 57 (1940) 1125;
see also S. Fernbach, R. Serber and T.B. Taylor - Phys. Rev. 75 (1949) 1.
17. M.M. Shapira - Phys.Rev. 90 (1953) 171.

18. See, e.g., S.J. Brodsky and J. Pumplin - Phys.Rev. 182 (1968) 1794.
19. M.S. Hussein - Phys.Rev. C30 (1984) 1962;
M.S. Hussein, A.J. Baltz and B.V. Carlson - Phys.Rep. 113 (1984) 133.
20. T. Udagawa and T. Tamura - Phys.Rev. C29 (1984) 1922;
T. Udagawa, B.T. Kim and T. Tamura - Phys.Rev. C32 (1985) 124.
21. M.A. Nagarajan and G.R. Satchler - to appear in Phys. Lett. B.
22. See, e.g., L.G. Arnold and B.C. Clark - Phys.Lett. 84B (1979) 46;
L.G. Arnold, R.L. Mercer and P. Schwandt - Phys.Rev. C23 (1981) 1949;
L.G. Arnold - Phys.Rev. C25 (1982) 936.
23. B.V. Carlson, M.P. Isidro Filho and M.S. Hussein - Phys. Rev.Lett. 53 (1984) 2222; Proc. of the V Encontro Nacional de Física de Energias Intermediárias, Gramado, R.S.; see also, R. Dymarz - Phys.Lett. 155B (1985) 5.
24. A.K. Kerman, H. McManus and R.M. Thaler - Ann.Phys. (NY) 8 (1959) 551.
For more recent reviews see: E.J. Moniz - in Nuclear Physics with Heavy-Ions and Mesosn, Les Houches, Session XXX, 1977, Ed.R. Balian (North-Holland); H. Feshbach - in Nuclear Physics with Heavy Ions and Mesons, Les Houches, Session XXX 1977, Ed.R. Balian (North-Holland).

25. J.M. Eisenberg and D.S. Koltun - Theory of Meson Interactions with Nuclei (J. Wiley & Sons, NY, 1980).

26. L. Ray - Phys.Rev. C20 (1979) 1857.

27. E. Boridy and H. Feshbach - Ann.Phys. (NY) 109 (1977) 468.

28. G.R. Satchler and W.G. Love - Phys.Rep. 55 (1979) 183.

29. R.A. Rego and M.S. Hussein - Phys.Rev. C in press.

30. K. Kikuchi and M. Kawai - Nuclear Matter and Nuclear Reactions (North-Holland Publishing Company, Amsterdam) (1968) 37.

31. E. Clementel and C. Villi - Nuovo Cimento II (1955) 176.

32. See, e.g., B. Sinha - Phys.Rep. 20C (1975) 1; Phys.Rev. Lett. 24 (1982) 209.

33. B.C. Clark et al. - Phys.Rev.Lett. 50 (1983) 1644; J.R. Shephard, J.A. McNeil and S.J. Wallace - Phys.Rev. Lett. 50 (1983) 1443.

34. J.A. McNeil, J.R. Shephard and S.J. Wallace - Phys.Rev. Lett. 50 (1983) 1439.

35. R.D. Amado, J. Piekarewicz, D.A. Sparrow and J.A. McNeil Phys.Rev. C28 (1983) 1663.

36. J. Friar and S.J. Wallace - Phys.Rev. C28 (1984) 2050.

37. The p+^{40}Ca and p+^{208}Pb alatex were collected from several references. See Ref. (23).

38. C.J. Horowitz - Nucl.Phys. A412 (1984) 228.

39. C. Bertulani - to be published and private communication.

TABLE CAPTIONS

Table 1. The parameters of the NN amplitude according to Eq. (III.24). From Ref. (26).

Table 2. The percentage transparancy for $^{12}C + ^{12}C$, $^{12}C + ^{208}Pb$, $^{40}Ca + ^{40}Ca$ and $^{208}Pb + ^{208}Pb$, at several center of mass energies. See text for details.

Table 3. The identical- particle correction of the total reaction cross sections of the systems $^{12}C + ^{12}C$, $^{40}Ca + ^{40}Ca$, $^{90}Zr + ^{90}Zr$ and $^{208}Pb + ^{208}Pb$. See text for details.

FIGURE CAPTIONS

Figure 1. The total cross section of the NN system vs laboratory energy (from Ref. 11).

Figure 2. The angle-integrated one-pion production cross section for the NN system (from Ref. 11).

Figure 3. The angle-integrated two-pion production cross-section for the NN system (from Ref. 11).

Figure 4. The transparency factor vs $\frac{2\lambda}{R}$ (Eq. (II.28)).

Figure 5. The correlation distance $R_{corr.}$ vs laboratory energy for the $p+^{12}C$ system. See text for details.

Figure 6. The real part of the second order nucleus-nucleus potential at four laboratory energies: 100 MeV/N (dashed curve), 200 MeV/A (dotted curve), 300 MeV (dashed-dotted curve) and 500 MeV (dashed-double dotted curve). For reference, the usual double-folding potential is also shown (full curve).

Figure 7. The imaginary part of the second-order nucleus-nucleus potential (same as Fig. 6). The potential equivalent to the double folding potential, namely Im "$t\rho,\rho_2$" is also exhibited (full curve).

Figure 8. The Pauli blocking-corrected total proton-proton cross section in the proton-nucleus system, for several values of R_{F_2} (the target Fermi momentum). Also shown is the free σ^T_{pp}.

Figure 9. Same as Fig. 8 for the neutron-proton total cross section in the proton-nucleus system.

Figure 10. Same as Fig. 8 in the nucleus-nucleus system.

Figure 11. Same as Fig. 9 in the nucleus-nucleus system.

Figure 12. The imaginary part of the "$t\rho_1\rho_2$" interaction for $^{12}C+^{12}C$: a) with Pauli blocking; b) without Pauli blocking.

Figure 13. Same as Fig. 12 for the $^{208}Pb+^{208}Pb$ system.

Figure 14. The total reaction cross section for $^{12}C+^{12}C$ vs E_{CM}/A. Full curve includes Pauli blocking plus refractive effects, dashed-dotted curve corresponds to $\bar{w}$ with no refractive effects, and dashed curve represents claculation with the free σ^T_{NN}. The data points were collected from the experimental papers cited in the reference list (Refs. 7-10).

Figure 15. Same as Fig. 14 for $^{12}C+^{208}Pb$.

Figure 16. Same as Fig. 14 for $^{208}Pb+^{208}Pb$.

Figure 17. Same as Fig. 14 for $^{12}C+^{40}Ca$ (no calculation with $\bar{w}$ only is shown; see text for details).

Figure 18. Same as Fig. 17 for $^{40}Ca+^{40}Ca$.

Figure 19. Same as Fig. 17 for $^{12}C+^{90}Zr$.

Figure 20. Same as Fig. 17 for $^{90}Zr+^{90}Zr$.

Figure 21. Same as Fig. 17 for $^{40}Ca+^{208}Pb$.

Figure 22. Same as Fig. 17 for $^{90}Zr+^{208}Pb$.

Figure 23. The imaginary phase shift calculated according to the WKB approximation (full curve) and the Eikonal approximation (dashed curve): a) $E_{C.M.}$=10 MeV, W_o=5 MeV; b) $E_{C.M.}$=10 MeV, W_o=50 MeV; c) $E_{C.M.}$=100 MeV, W_o=5 MeV; d) $E_{C.M.}$=100 MeV, W_o=50 MeV.

Figure 24. Total reaction cross-section for $p+^{40}Ca$ calculated with the relativistic, Dirac, description (Appendix II). The data points were taken from the references cited in Ref. (23).

Figure 25. Same as Fig. 24 for $p+^{208}Pb$.

Figure 26. The geometrical realization of Pauli blocking in the nucleon-nucleus system: a) restrictions on the momentum vectors; b) the allowed scattering sphere and c) the Pauli forbidden region (dashed area). See Appendix IV for details.

Figure 27. Same as Fig. 26 for the nucleus-nucleus system: a) the three "spheres" describing the scattering region in momentum space, and b) the Pauli forbidden region (dashed area). See Appendix IV for details.

E_{LAB} (MeV)	σ^T_{pp} (mb)	α_{pp}	a_{pp} (fm^2)	σ^T_{pn} (mb)	α_{pn}	a_{pn} (fm^2)
100	33.2	1.87	0.66	72.7	1.00	0.36
150	26.7	1.53	0.57	50.2	0.96	0.58
200	23.6	1.15	0.56	42.0	0.71	0.68
325	24.5	0.45	0.26	36.1	0.16	0.36
425	27.4	0.47	0.21	33.2	0.25	0.27
550	36.9	0.32	0.04	35.5	-0.24	0.085
650	42.3	0.16	0.07	37.7	-0.35	0.09
800	47.3	0.06	0.09	37.9	-0.20	0.12
1000	47.2	-0.09	0.09	39.2	-0.46	0.12
2200	44.7	-0.17	0.12	42.0	-0.50	0.14

TABLE I

TABLE II

$^{12}C + {}^{12}C$ *	
$\frac{E_{c.m.}}{A}\left(\frac{MeV}{nucleon}\right)$	T
50	46,7%
100	50,9%
200	49,0%
300	47,8%
500	44,0%

* r_o = 1,57 fm

$^{12}C + {}^{208}Pb$ *	
$\frac{E_{c.m.}}{A}\left(\frac{MeV}{nucleon}\right)$	T
50	34,4%
100	32,2%
200	35,4%
500	32,9%
900	25,2%

* r_o = 1,50 fm

$^{40}Ca + {}^{40}Ca$ *	
$\frac{E_{c.m.}}{A}\left(\frac{MeV}{nucleon}\right)$	T
50	28,9%
100	32,4%
200	31,1%
300	30,0%
500	27,2%

* r_o = 1,50 fm

$^{208}Pb + {}^{208}Pb$ *	
$\frac{E_{c.m.}}{A}\left(\frac{MeV}{nucleon}\right)$	T
50	26,2%
100	29,1%
200	28,2%
300	27,1%
500	25,5%

* r_o = 1,50 fm

$E_{Lab./A}$ (MeV)	$^{12}C + {}^{12}C$		$^{40}Ca + {}^{40}Ca$		$^{90}Zr + {}^{90}Zr$		$^{208}Pb + {}^{208}Pb$	
	b_c (fm)	$\Delta\sigma_s$ (fm^2)	b_c	$\Delta\sigma_s$ (fm^2)	b_c	$\Delta\sigma_s$ (fm^2)	b_c	$\Delta\sigma_s$ (fm^2)
2	5.5	-8.56	5.0	-4.28	5.0	-0.03	4.0	0.44
4	5.5	12.28	5.0	-2.24	5.0	-0.85	4.0	-0.37
6	5.5	-11.29	6.5	0.14	6.5	-1.29	4.0	0.27
8	5.5	7.97	7.0	-3.46	7.0	-0.61	6.0	0.44
10	5.5	-3.4	7.0	2.71	8.0	-0.52	8.5	0.74
12	5.5	-4.49	7.0	-2.75	8.5	0.46	9.0	-0.69
14	5.5	6.72	7.0	2.23	8.5	-1.45	9.5	-0.46
16	5.5	-1.07	7.5	-2.53	9.0	1.31	10.0	-0.69
18	5.5	-6.09	7.5	1.15	9.0	1.35	11.0	-0.48
20	5.5	2.11	7.5	2.37	10.0	-0.19	12.0	0.72
22	5.5	4.6	8.0	0.89	10.0	1.2	15.0	0.54
24	5.5	3.8	8.0	1.45	12.0	-1.12	15.0	0.42

TABLE III

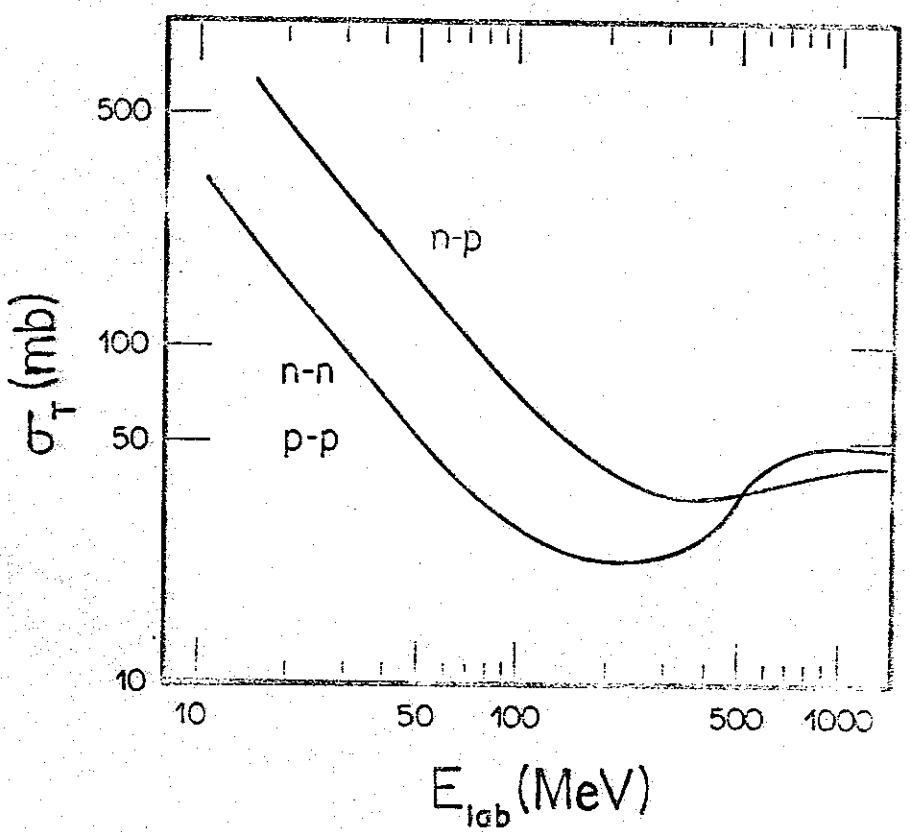
σ_T (mb)
500
100
50
10
n-p
n-n
p-p
10
50
100
500
1000
E_{lab} (MeV)

Fig. 1

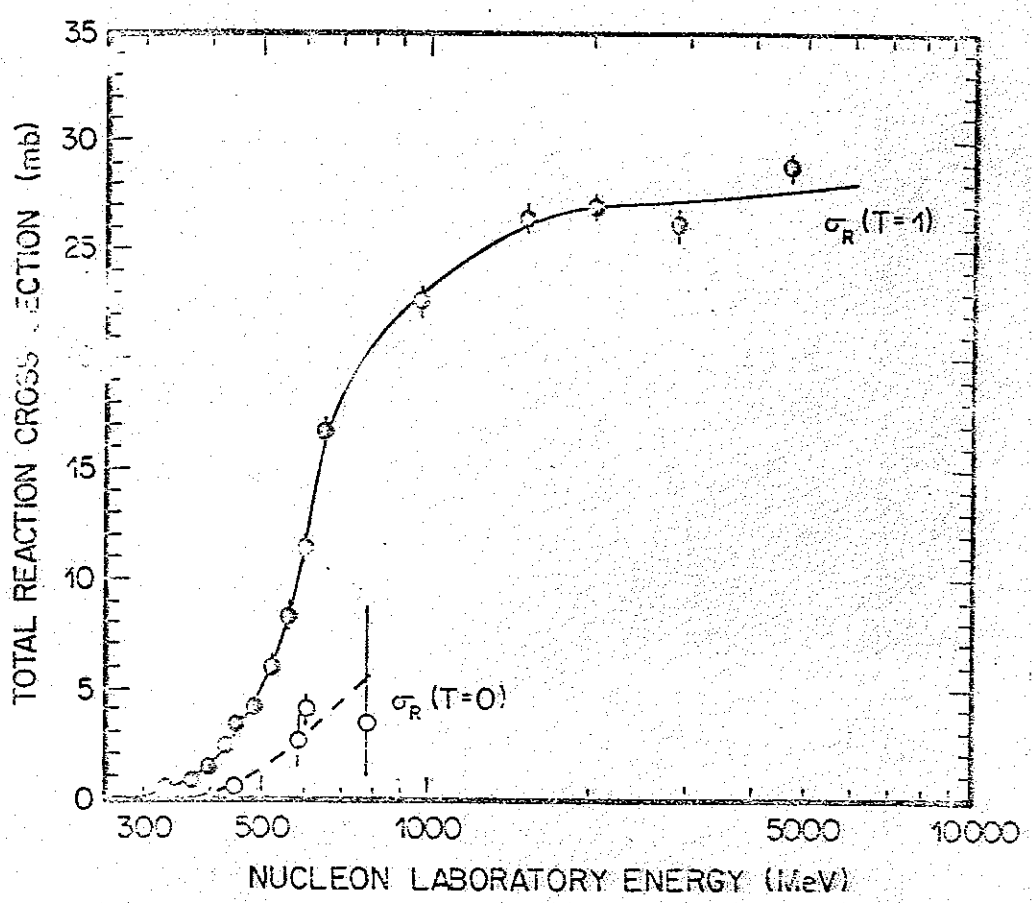
TOTAL REACTION CROSS SECTION (mb)
35
30
25
15
10
5
0
σ_R (T=1)
σ_R (T=0)
300
500
1000
5000
10000
NUCLEON LABORATORY ENERGY (MeV)

Fig. 2

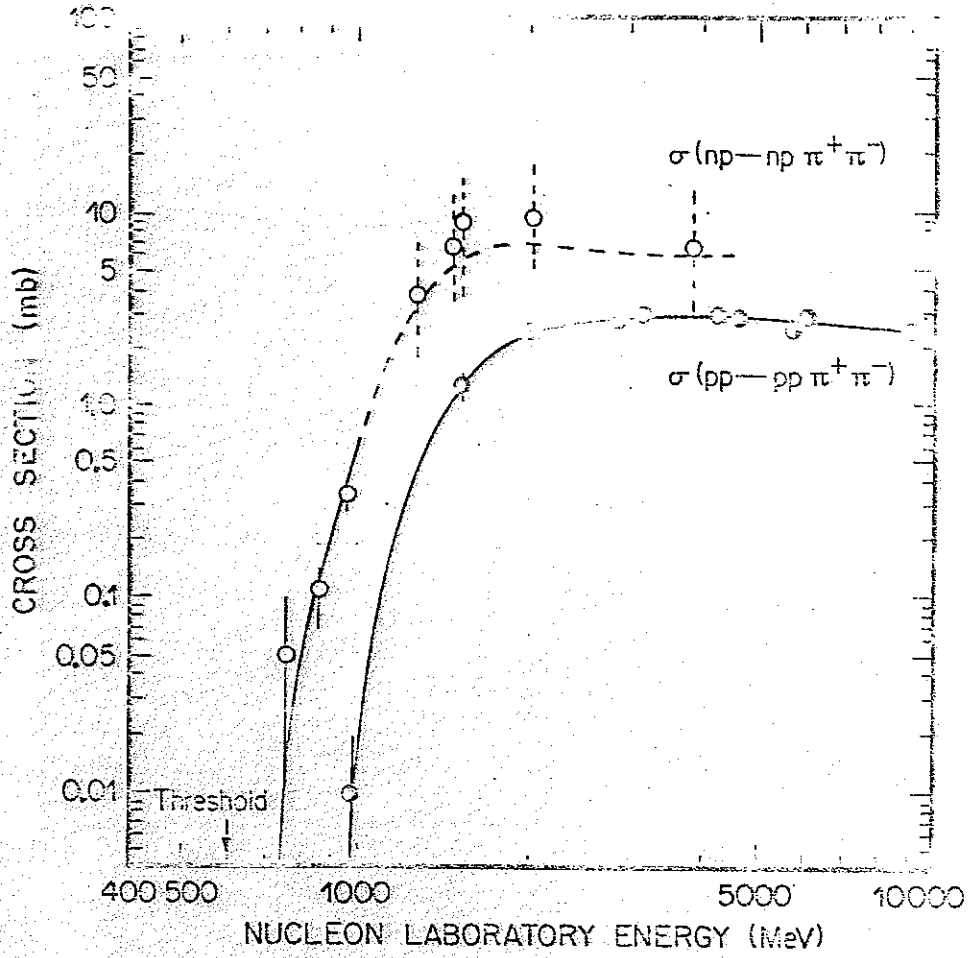
CROSS SECTION (mb)
50
10
5
0.5
0.1
0.05
0.01
σ (np— np π+π−)
σ (pp— pp π+π−)
Threshold
400 500
1000
5000
10000
NUCLEON LABORATORY ENERGY (MeV)

Fig. 3

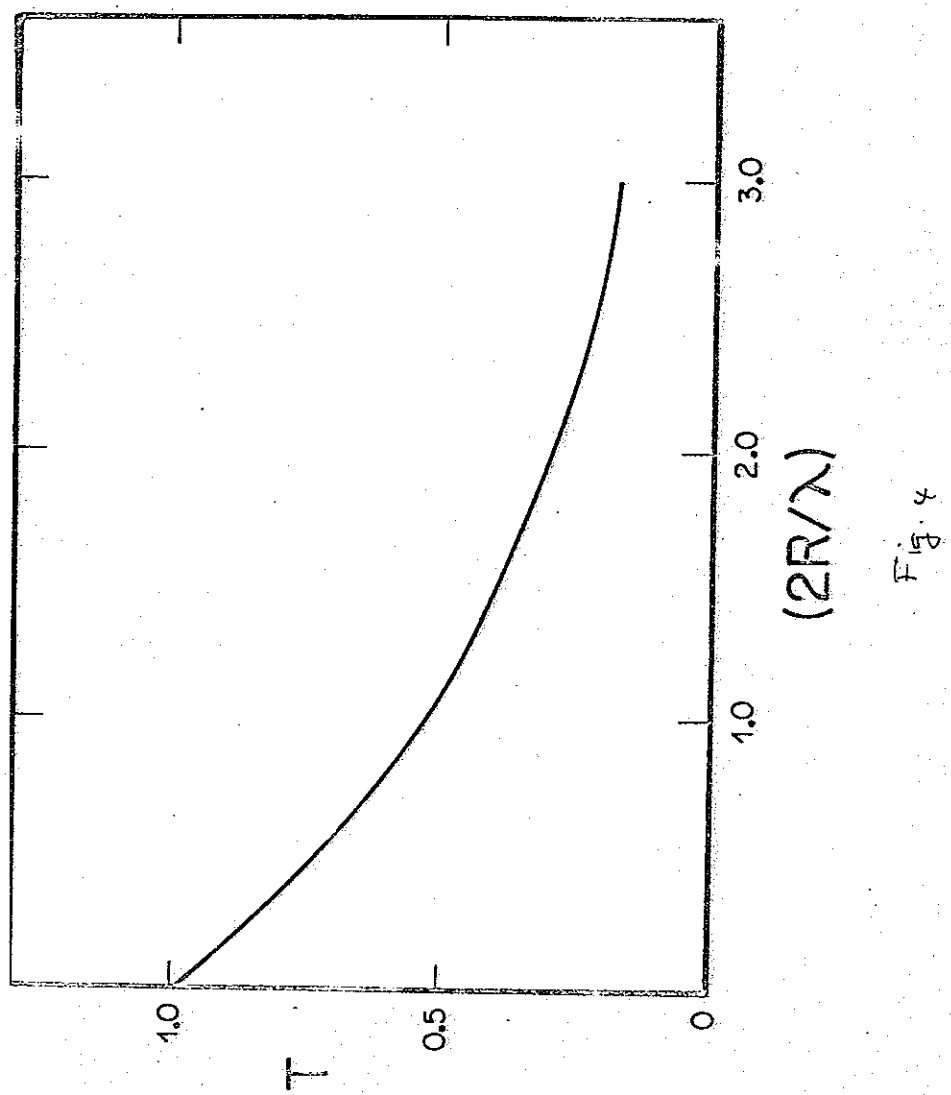
T
1.0
0.5
0
(2R/λ)
1.0
2.0
3.0

Fig. 4

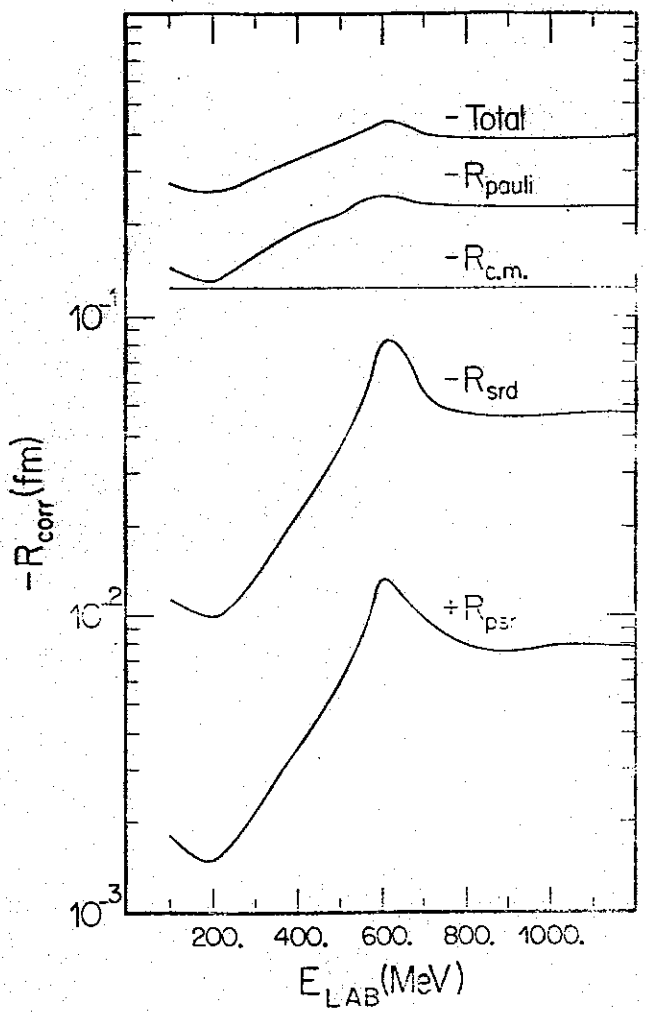
- Total
$-R_{pauli}$
$-R_{c.m.}$
$-R_{srd}$
$+R_{psr}$
$-R_{corr}$ (fm)
10^{-1}
10^{-2}
10^{-3}
200. 400. 600. 800. 1000.
E_{LAB}(MeV)

Fig.5

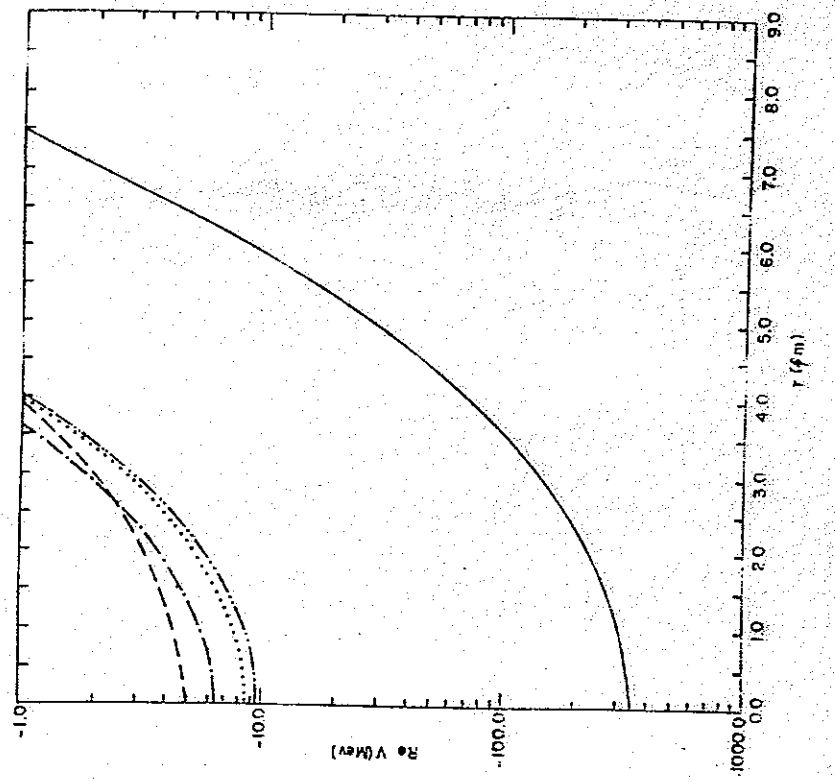
-1.0
-10.0
-100.0
-1000.0
R• V(MeV)
0.0
1.0
2.0
3.0
4.0
5.0
6.0
7.0
8.0
9.0
r (fm)

Fig.6

Fig. 7

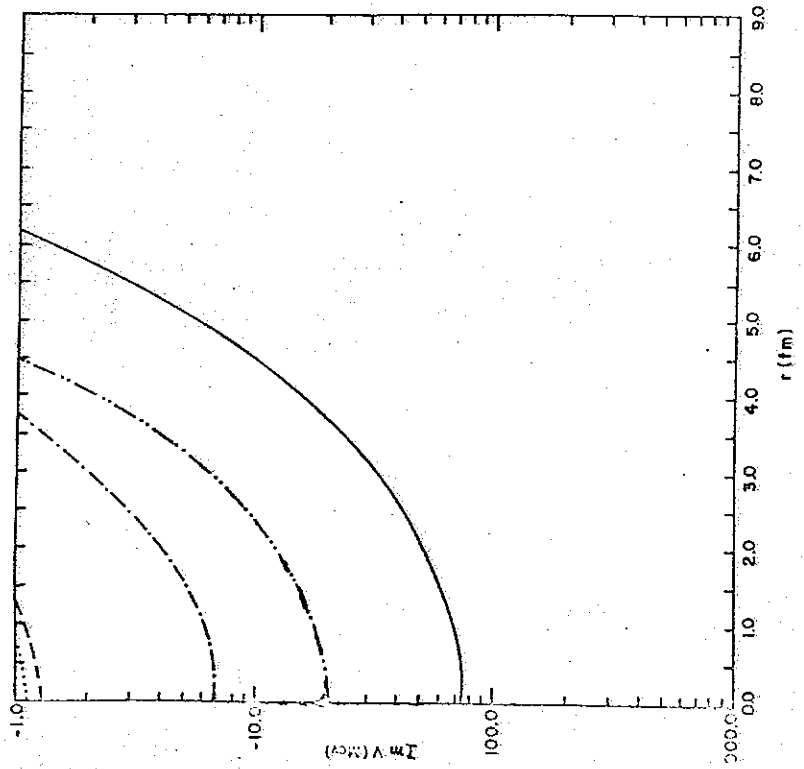

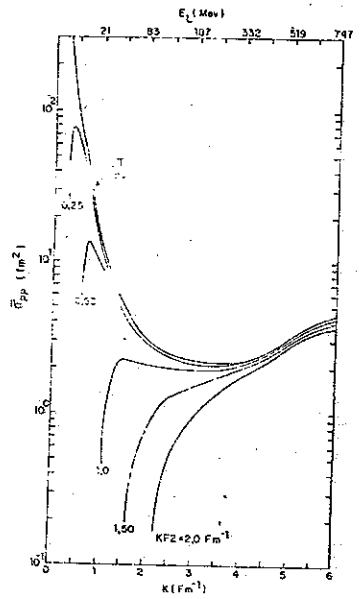

Fig 8

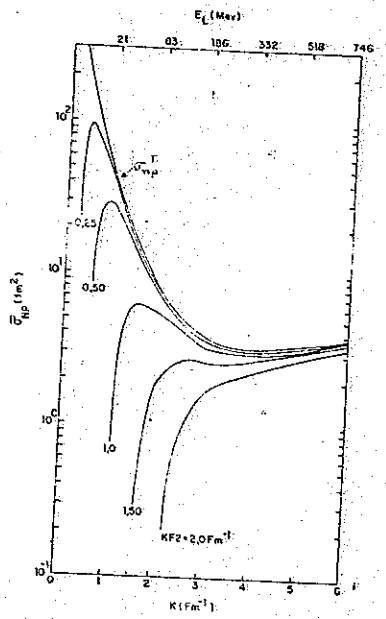

Fig 9

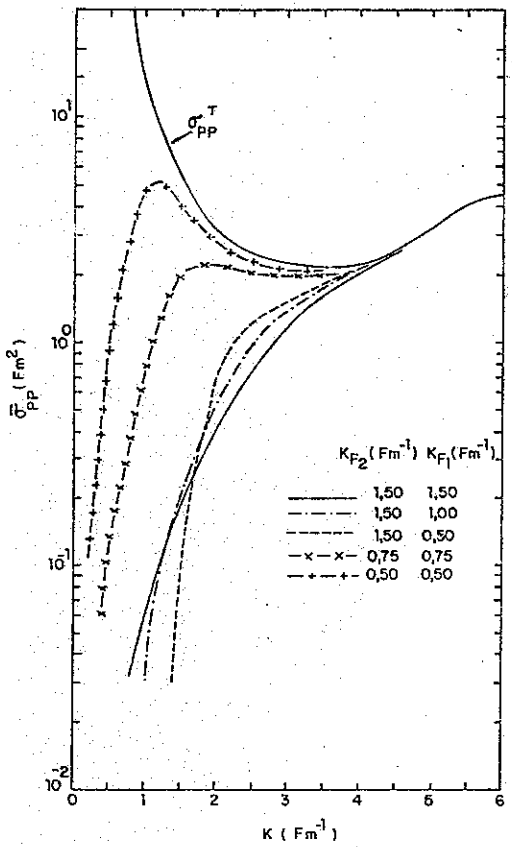
σ^T_{PP}
$\bar{\sigma}_{PP}$ (Fm^2)
K (Fm^{-1})
K_{F_2}(Fm^{-1}) K_{F_1}(Fm^{-1})
1,50 1,50
1,50 1,00
1,50 0,50
0,75 0,75
0,50 0,50

Fig. 10

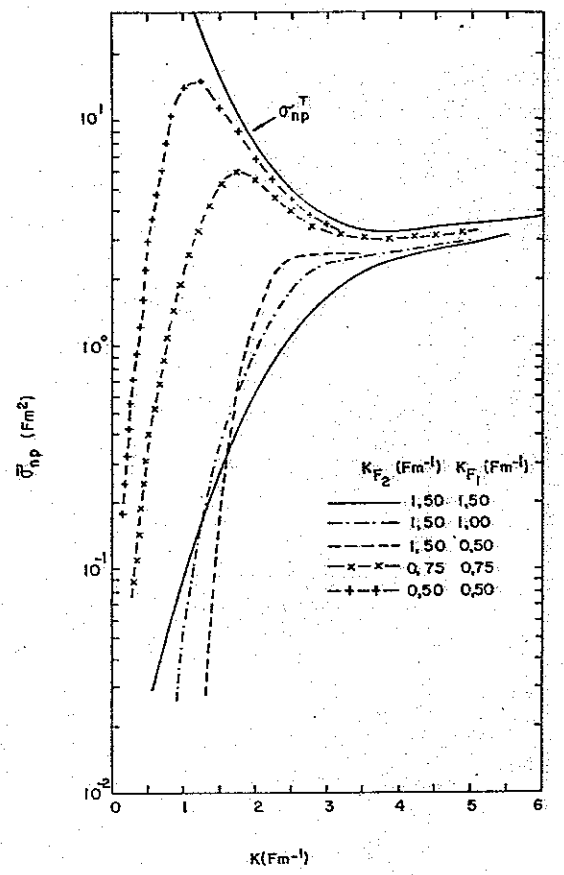
σ^T_{np}
$\bar{\sigma}_{np}$ (Fm^2)
K(Fm^{-1})
K_{F_2} (Fm^{-1}) K_{F_1} (Fm^{-1})
1,50 1,50
1,50 1,00
1,50 0,50
0,75 0,75
0,50 0,50

Fig. 11

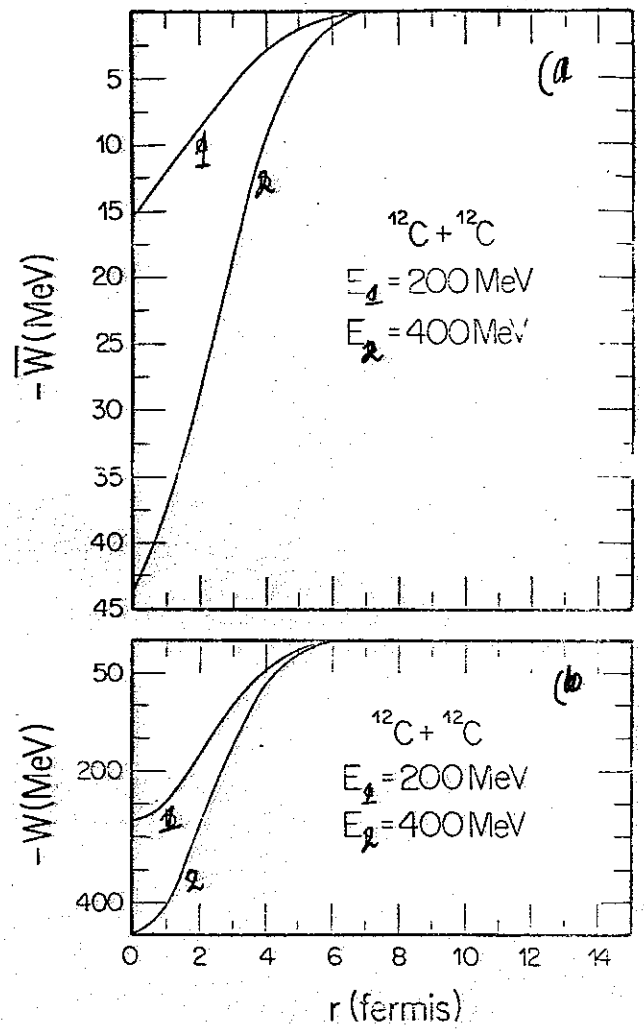
(a
$^{12}C + ^{12}C$
$E_1 = 200$ MeV
$E_2 = 400$ MeV
$-\overline{W}$ (MeV)
5
10
15
20
25
30
35
40
45
(b
$^{12}C + ^{12}C$
$E_1 = 200$ MeV
$E_2 = 400$ MeV
$-W$ (MeV)
50
200
400
0 2 4 6 8 10 12 14
r (fermis)

Fig. 12

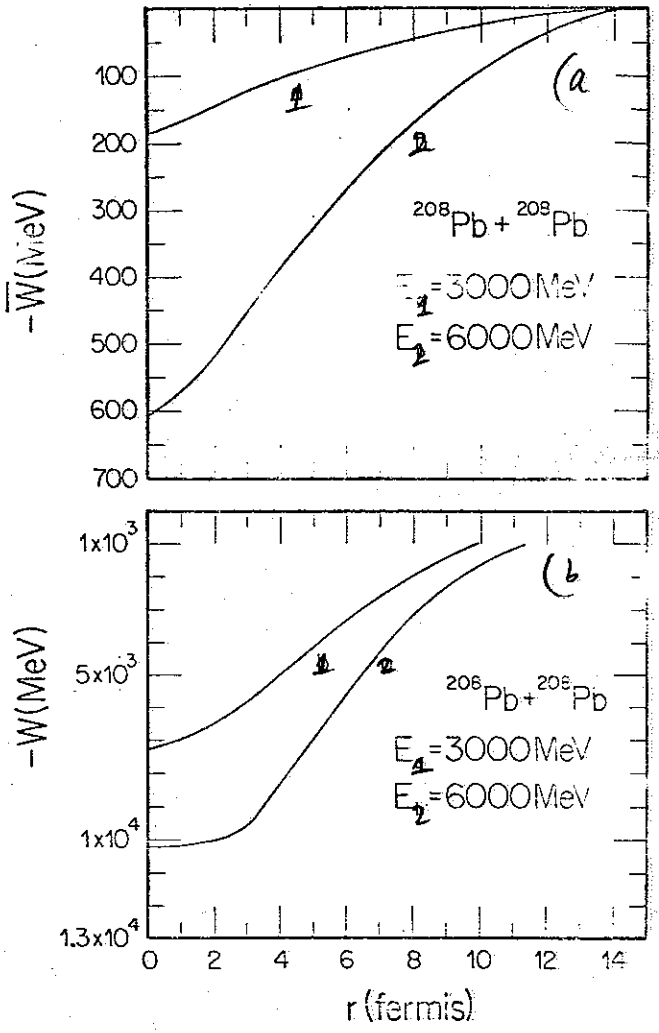
(a
$^{208}Pb + ^{208}Pb$
$E_1 = 3000$ MeV
$E_2 = 6000$ MeV
$-\overline{W}$ (MeV)
100
200
300
400
500
600
700
(b
$^{208}Pb + ^{208}Pb$
$E_1 = 3000$ MeV
$E_2 = 6000$ MeV
$-W$ (MeV)
$1x10^3$
$5x10^3$
$1x10^4$
$1.3x10^4$
0 2 4 6 8 10 12 14
r (fermis)

Fig. 13

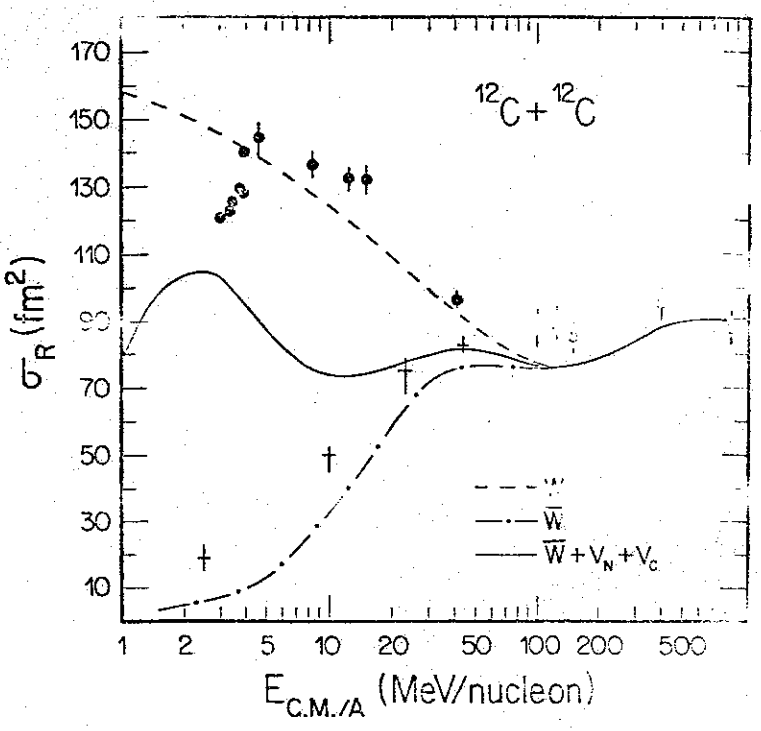
$^{12}C+^{12}C$
σ_R (fm^2)
$E_{C.M./A}$ (MeV/nucleon)
W
$\overline{W}$
$\overline{W}+V_N+V_c$

Fig. 14

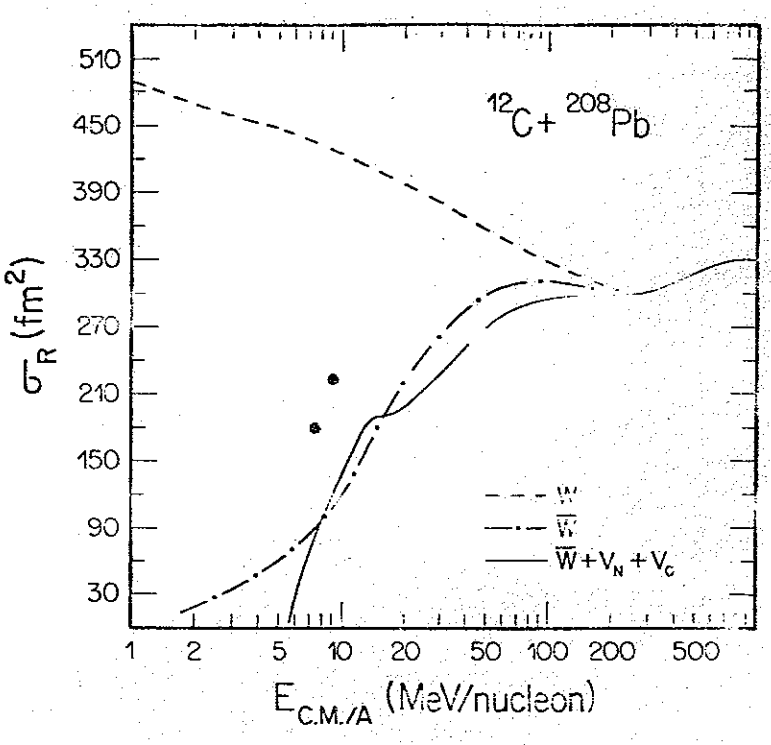
$^{12}C+^{208}Pb$
σ_R (fm^2)
$E_{C.M./A}$ (MeV/nucleon)
W
$\overline{W}$
$\overline{W}+V_N+V_c$

Fig. 15

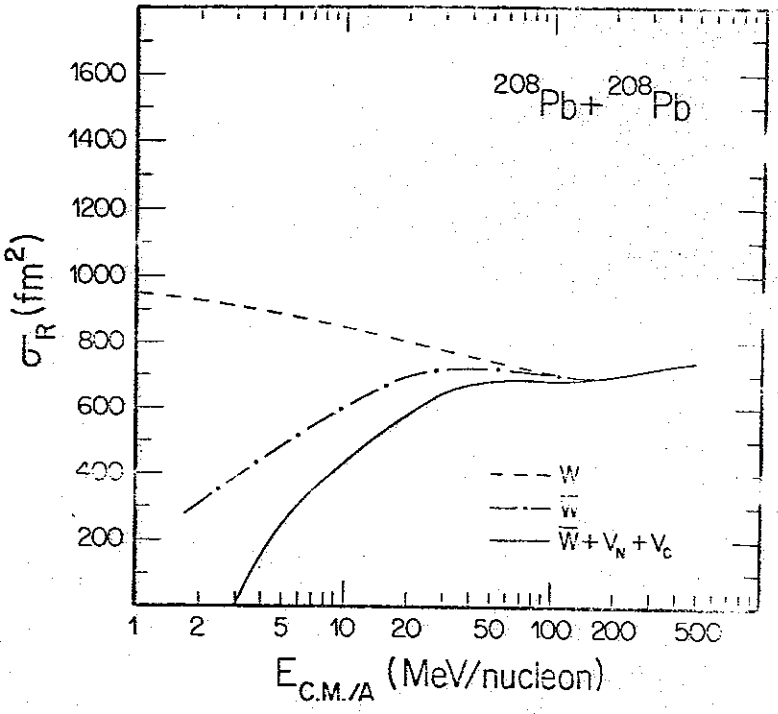
$^{208}Pb + ^{208}Pb$
σ_R (fm^2)
1600
1400
1200
1000
800
600
400
200
W
$\overline{W}$
$\overline{W} + V_N + V_c$
1 2 5 10 20 50 100 200 500
$E_{C.M./A}$ (MeV/nucleon)

Fig. 16

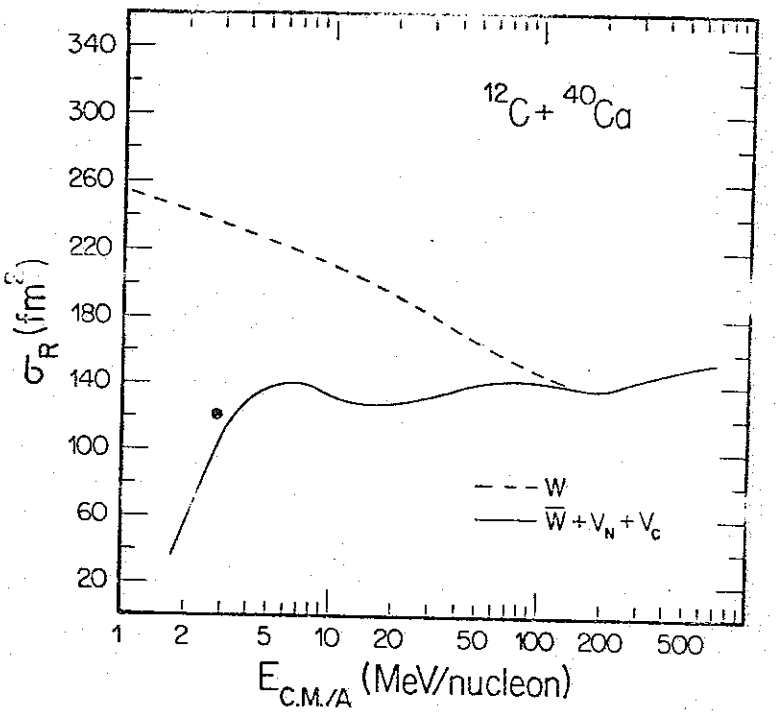
$^{12}C + ^{40}Ca$
σ_R (fm^2)
340
300
260
220
180
140
100
60
20
W
$\overline{W} + V_N + V_c$
1 2 5 10 20 50 100 200 500
$E_{C.M./A}$ (MeV/nucleon)

Fig. 17

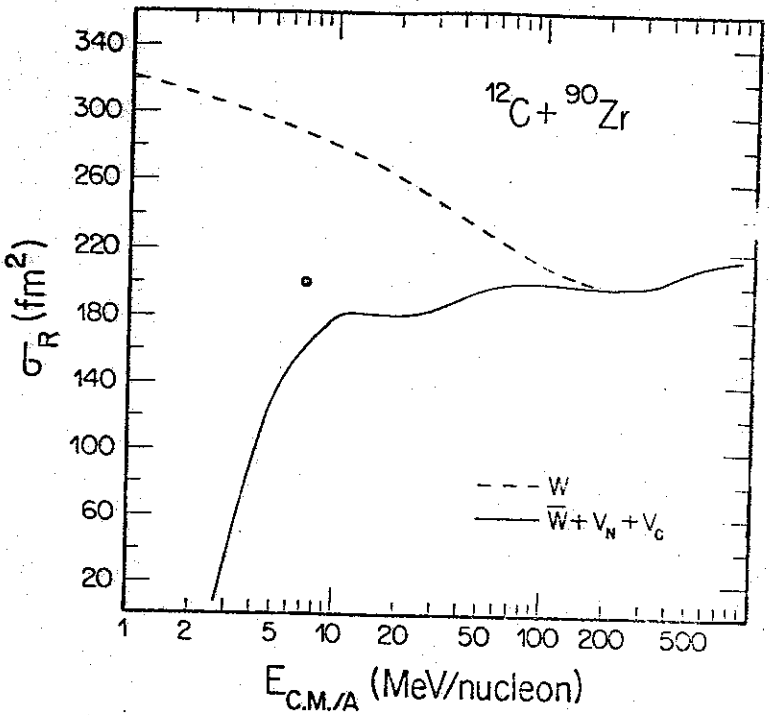
$^{12}C + ^{90}Zr$
σ_R (fm^2)
340
300
260
220
180
140
100
60
20
1
2
5
10
20
50
100
200
500
$E_{C.M./A}$ (MeV/nucleon)
W
$\bar{W} + V_N + V_C$

Fig. 18

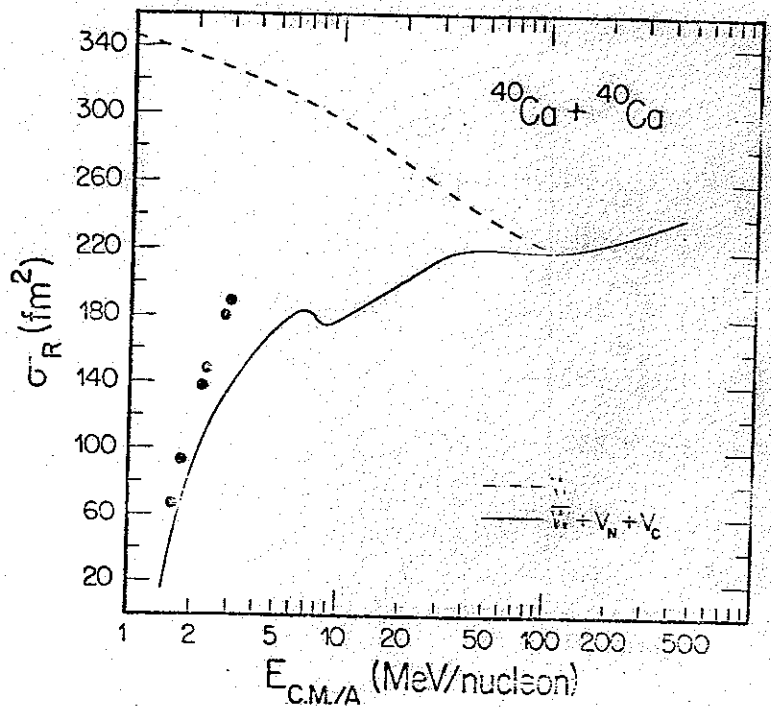
$^{40}Ca + ^{40}Ca$
σ_R (fm^2)
340
300
260
220
180
140
100
60
20
1
2
5
10
20
50
100
200
500
$E_{C.M./A}$ (MeV/nucleon)
$\bar{W} + V_N + V_C$

Fig. 19

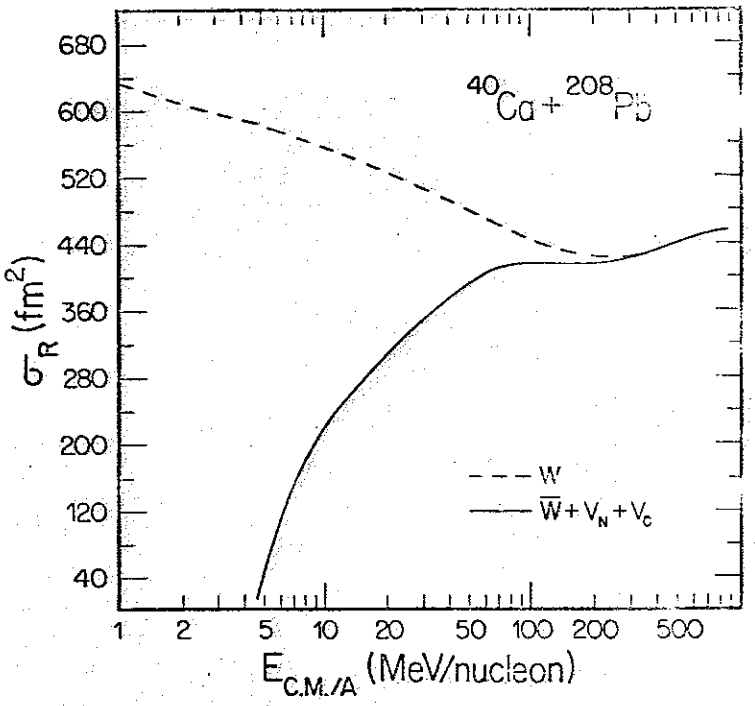
680
600
520
440
360
280
200
120
40
σ_R (fm^2)
$^{40}Ca + ^{208}Pb$
W
$\bar{W} + V_N + V_c$
1
2
5
10
20
50
100
200
500
$E_{C.M./A}$ (MeV/nucleon)

Fig. 20

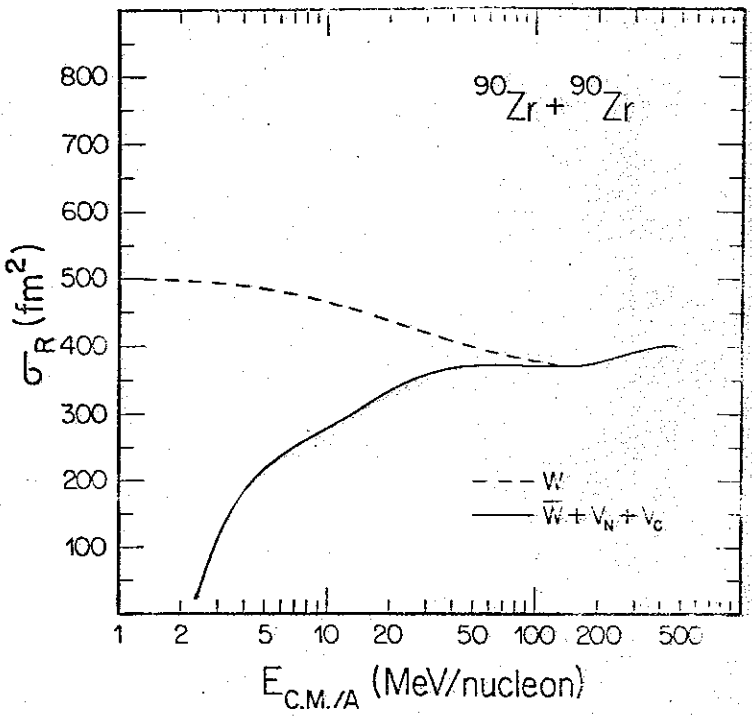
800
700
600
500
400
300
200
100
σ_R (fm^2)
$^{90}Zr + ^{90}Zr$
W
$\bar{W} + V_N + V_c$
1
2
5
10
20
50
100
200
500
$E_{C.M./A}$ (MeV/nucleon)

Fig. 21

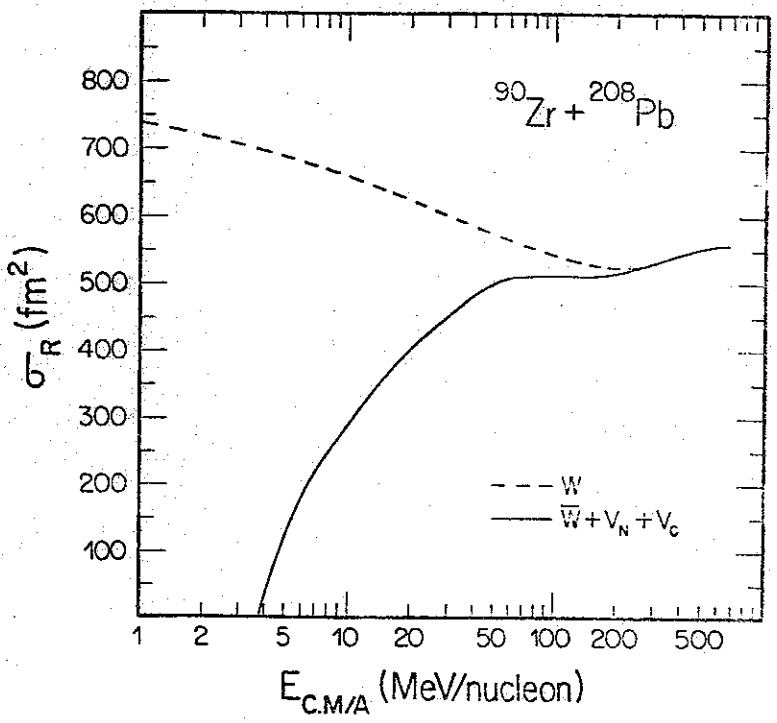

Fig. 22

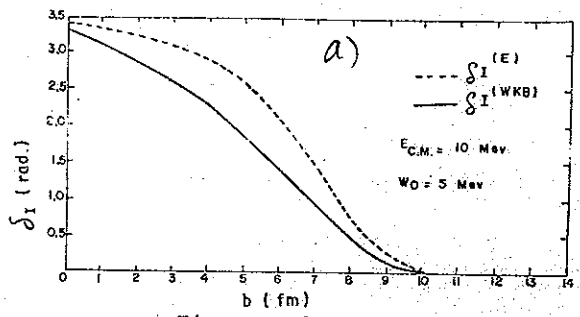

Figura E.1

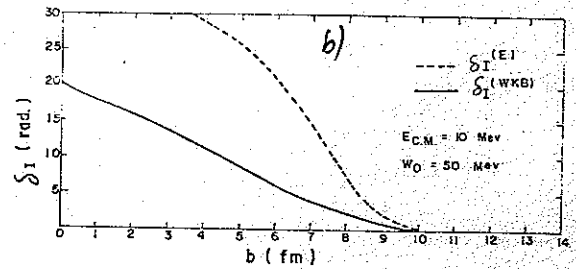

Figura E.2

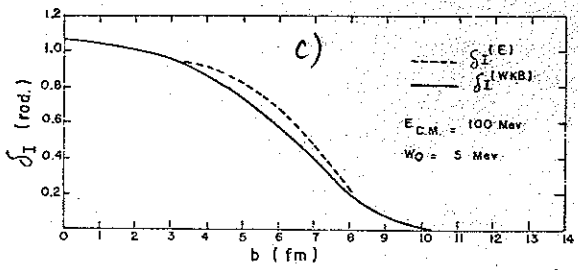

Figura E.3

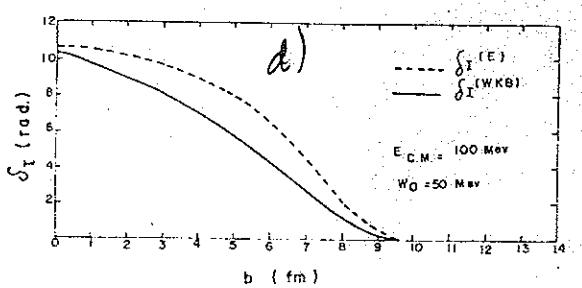

Fig. 23

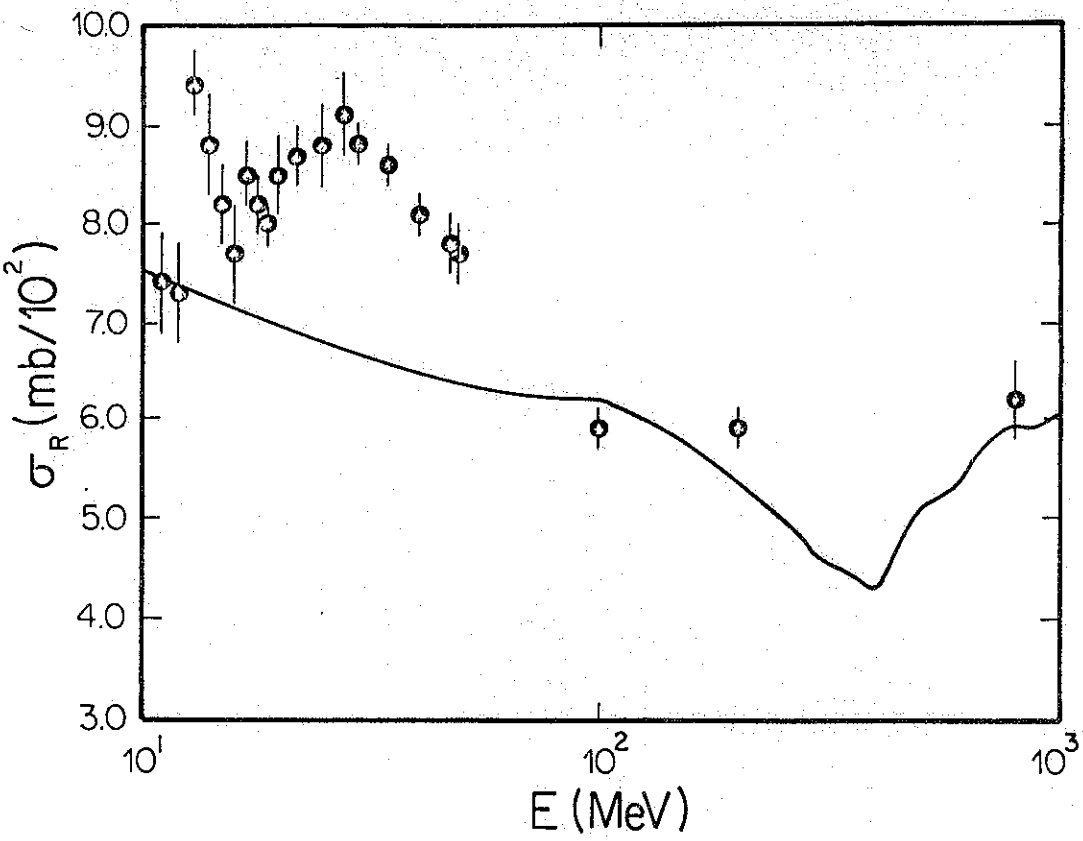
10.0
9.0
8.0
7.0
6.0
5.0
4.0
3.0
σ_R (mb/10^2)
10^1
10^2
10^3
E (MeV)

Fig. 2a

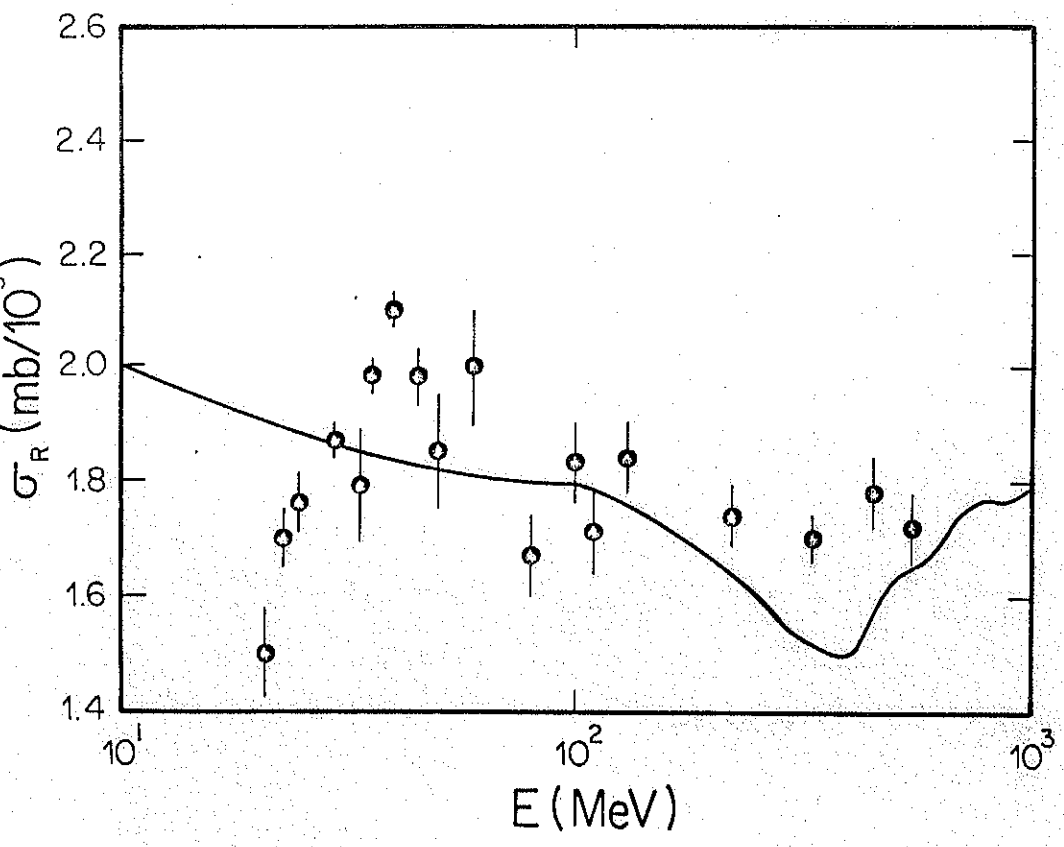
2.6
2.4
2.2
2.0
1.8
1.6
1.4
σ_R (mb/10^3)
10^1
10^2
10^3
E (MeV)

Fig. 2b

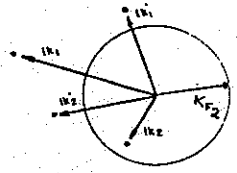

a)

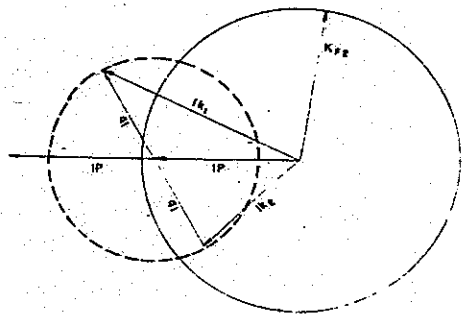

b)

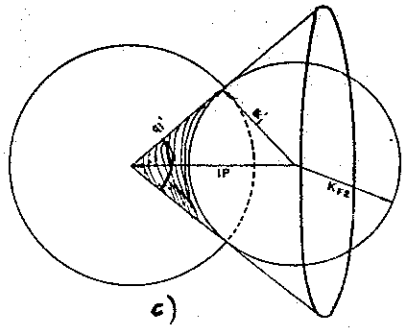

c)

Fig. 26

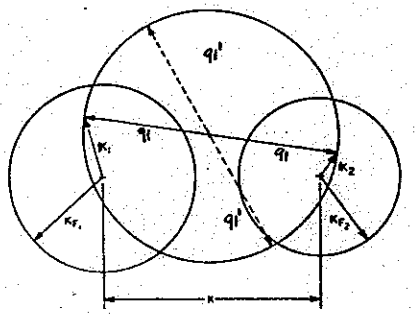

a)

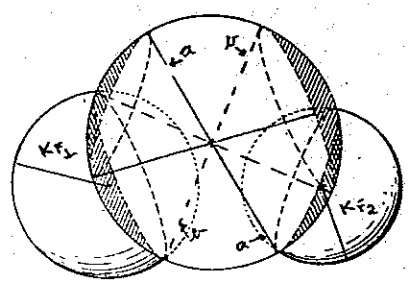

b)

Fig. 27.